2022 1st Season Stock Assessment

Falkland calamari

(*Doryteuthis gahi*)

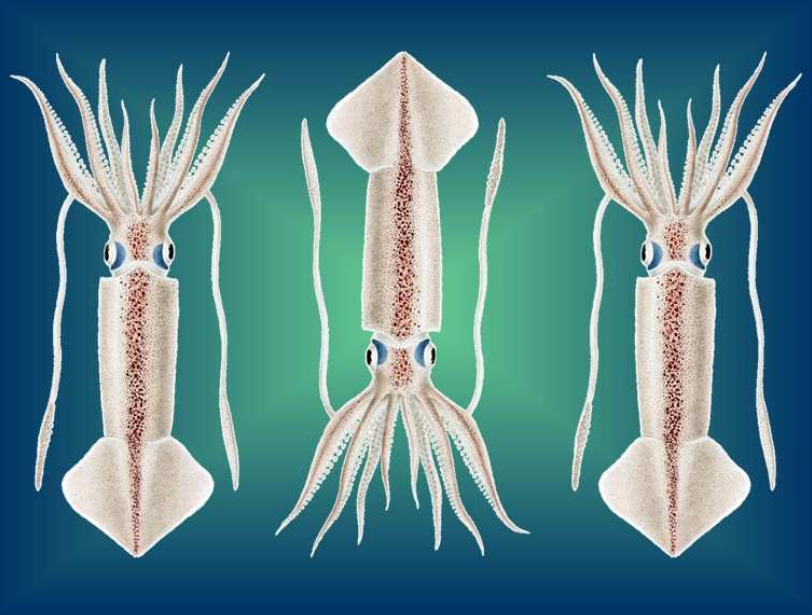

S1 - 2022 - LOL

Andreas Winter · Frane Skeljo

Natural Resources - Fisheries
Falkland Islands Government
Stanley, Falkland Islands

August 2022

Index

Summary

1) The 2022 first season *Doryteuthis gahi* fishery (C license) was open from February 23rd and closed by directed order on April 27th. Compensatory flex days for mechanical breakdown and bad weather resulted in 19 vessel-days taken after April 27th, with the last vessel fishing as late as May 1st.
2) 56,417 tonnes of *D. gahi* catch were reported in the 2022 C-license fishery, giving an average CPUE of 58.4 t vessel-day^{-1}. Total catch and CPUE were the second-highest for a first season since 2004, following 2021. 43.1% of *D. gahi* catch and 43.2% of fishing effort were taken south of 52º S; 56.9% of *D. gahi* catch and 56.8% of fishing effort were taken north of 52º S. One vessel was licensed to fish experimentally north of the Loligo Box for three days; that catch and effort was calculated as part of the north sub-area.
3) In the south sub-area, four depletion periods / immigration peaks were inferred on February 23rd (start of the season), March 2nd, March 15th, and April 19th. In the north sub-area, three depletion periods / immigrations were inferred on February 23rd, February 27th, and March 3rd.
4) Approximately 195,855 tonnes of *D. gahi* (95% confidence interval: 163,981 to 519,171 t) were estimated to have immigrated into the Loligo Box after the start of first season 2022, of which 147,798 t in the south sub-area and 48,056 t in the north sub-area.
5) The escapement biomass estimate for *D. gahi* remaining in the Loligo Box at the end of first season 2022 was: Maximum likelihood of 93,275 tonnes, with a 95% confidence interval of 81,579 to 304,984 tonnes.
   The risk of *D. gahi* escapement biomass at the end of the season being less than 10,000 tonnes was estimated at effectively zero.

Introduction

First season (C licence) of the 2022 *Doryteuthis gahi* fishery (Patagonian longfin squid – colloquially *Loligo*) opened on February 23rd, with 15 vessels entering the fishery. One vessel postponed its entry for a day to deal with a mechanical issue. Throughout the season, 29 flex days were requested by all except one vessel, for mechanical breakdowns and bad weather (of which 15 on March 14th, and 6 on April 28th; Figure 1). A total of 19 fishing days were taken after scheduled closure on April 27th with the last vessel fishing on May 1st.

Because of small sizes of the *D. gahi* squid, the Loligo Producers Group proposed and cooperated with closure of the southern part of the Loligo Box[a] on four occasions: from 0001 hours on February 23rd, for 7 days, from 0001 hours on March 5th, for 7 days, from 0001 hours on March 12th, for 3 days, and from 0001 hours on March 18th, for 5 days. In parallel, one vessel was authorized under experimental licence (FK033E22) to test-fish 3 grids adjacent to the northern boundary of the Loligo Box for three days, March 6th to March 8th (Figure 2). For assessment, these experimental fishing days were included as regular season catches and effort in the north sub-area.

All C-license vessels were required to embark an observer tasked to monitor presence and incidental capture of pinnipeds. Seal Exclusion Devices were mandated north of 52° 30' S latitude on February 26th[b], following reported two pinniped trawl mortalities, and mandated south of 52° 30' S latitude on March 3rd[c], following two further pinniped trawl mortalities.

[a] South of 52° 30' S latitude, different from the statutory 52° S latitude north – south sub-area demarcation.
[b] From next shot as of 13:17 FT.
[c] From next shot as of 21:11 FT.

Total reported *D. gahi* catch under first season C licence was 24,342.3 south + 32,074.7 north = 56,417.0 tonnes, corresponding to an average CPUE of 56417 / 966 = 58.4 tonnes vessel-day^{-1}. Both total catch and average CPUE were second-highest among first seasons, after 2021 (Table 1).

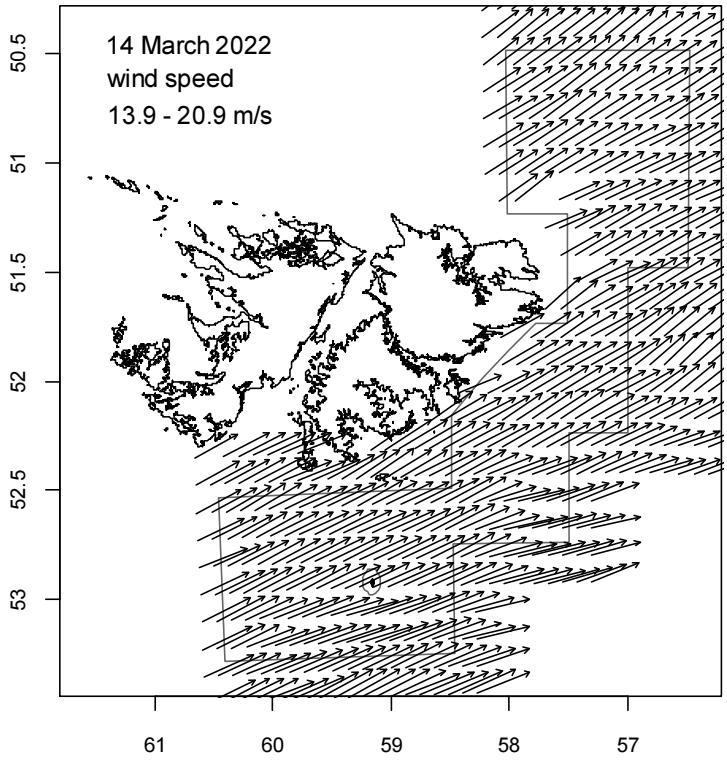

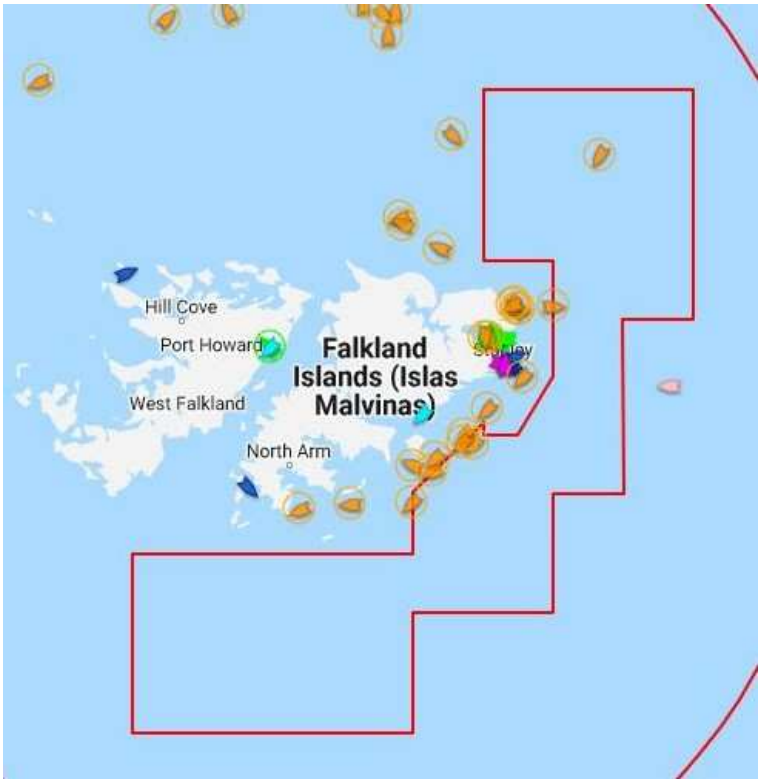

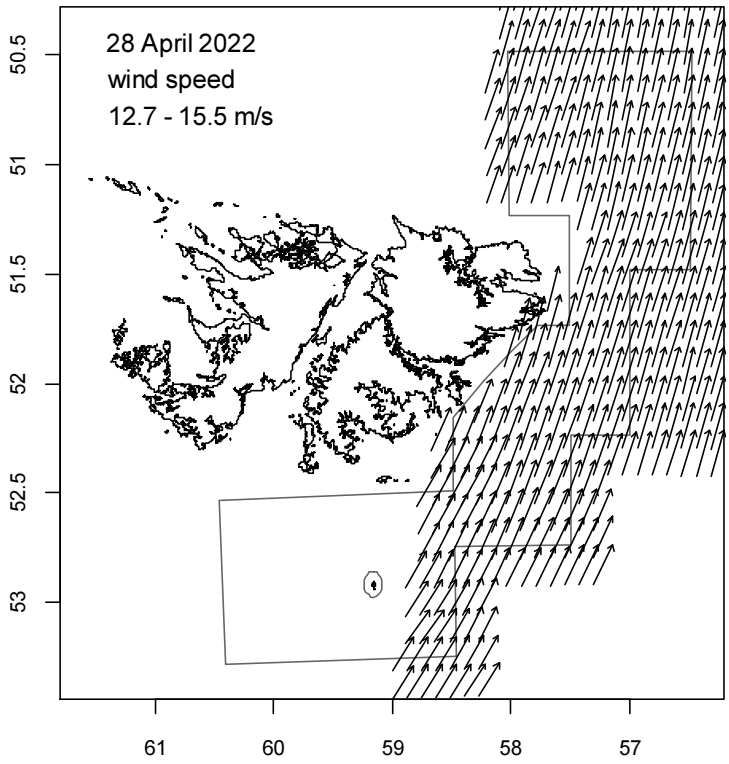

Figure 1 [previous page]. Fish Ops chart display (Big Ocean Data) (right) and wind speed vector plots (Copernicus Marine Service) (left) on March 14th, when only one vessel fished, and April 28th, when eight vessels fished.

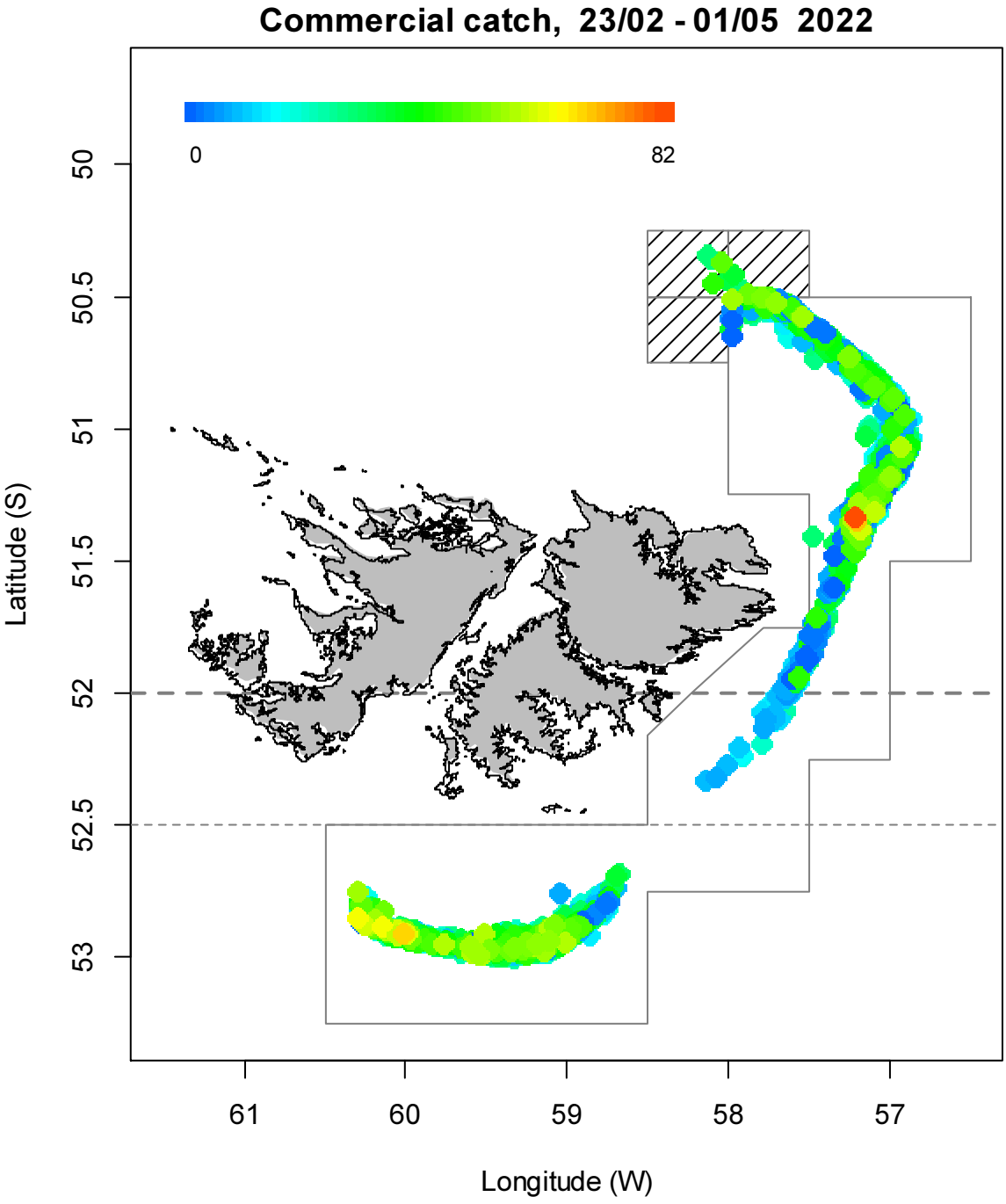

Figure 2. Spatial distribution of *D. gahi* 1st-season trawls, colour-scaled to catch weight (max. = 82.0 tonnes). 2445 trawl catches were taken during the season. In grey: the 'Loligo Box' fishing zone, 52 ºS parallel delineating the boundary between north and south assessment sub-areas (heavy broken line), 52.5 ºS parallel delineating the temporary south exclusion zone (thin broken line). Shaded diagonally: three additional grids in the north temporarily opened for exploratory fishing.

Table 1. *D. gahi* season comparisons since 2004, when catch management was assumed by the FIFD. Days: total number of calendar days open to licensed *D. gahi* fishing including (since 1st season 2013) optional flex days; V-Days: aggregate number of licensed *D. gahi* fishing days reported by all vessels for the season. Entries in italics are seasons closed by emergency order.

	Season 1			Season 2		
	Catch (t)	Days	V-Days	Catch (t)	Days	V-Days
2004	7,152	46	625	17,559	78	1271
2005	24,605	45	576	29,659	78	1210
2006	19,056	50	704	*23,238*	*53*	*883*
2007	17,229	50	680	*24,171*	*63*	*1063*
2008	24,752	51	780	26,996	78	1189
2009	12,764	50	773	*17,836*	*59*	*923*
2010	28,754	50	765	36,993	78	1169
2011	15,271	50	771	*18,725*	*70*	*1099*
2012	34,767	51	770	35,026	78	1095
2013	19,908	53	782	19,614	78	1195
2014	28,119	59	872	19,630	71	1099
2015	*19,383*	*57*	*871*[A]	*10,190*	*42*	*665*
2016	22,616	68	1020	23,089	68	1004
2017	39,433	68	999[B]	24,101	69	1002[C]
2018	43,085	69	975	35,828	68	977
2019	55,586	68	953	*24,748*	*43*	*635*
2020	29,116	68	1012	29,759	69	993
2021	*59,587*	*62*	*891*	34,750	68	982[D]
2022	56,417	68	966[E]			

[A] Does not include C-license catch or effort after the target was switched from *D. gahi* to *Illex*.
[B] Includes two vessel-days of experimental fishing for juvenile toothfish.
[C] Includes one vessel-day of experimental fishing for juvenile toothfish.
[D] Includes three vessel-days of experimental fishing for SED improvement.
[E] Includes three vessel-days of exploratory fishing north of the Loligo Box.

Assessment of the Falkland Islands *D. gahi* stock was conducted with depletion time-series models as in previous seasons (Agnew et al. 1998, Roa-Ureta and Arkhipkin 2007, Arkhipkin et al. 2008), and in other squid fisheries (cited in Arkhipkin et al. 2021). Because *D. gahi* has an annual life cycle (Patterson 1988, Arkhipkin 1993), stock cannot be derived from a standing biomass carried over from prior years (Rosenberg et al. 1990, Pierce and Guerra 1994). The depletion model instead calculates an estimate of population abundance over time by evaluating what levels of abundance and catchability must be present to sustain the observed rate of catch. Depletion modelling of the *D. gahi* target fishery is used both in-season and for post-season analysis, with the objective of maintaining an escapement biomass of 10,000 tonnes *D. gahi* at the end of each season as a conservation threshold (Agnew et al. 2002, Barton 2002).

Methods

The depletion model formulated for the Falklands *D. gahi* stock is based on the equivalence:

$$C_{day} = q \times E_{day} \times N_{day} \times e^{-M/2} \quad \textbf{(1)}$$

where q is the catchability coefficient, M is the natural mortality rate (considered constant at 0.0133 day^{-1}; Roa-Ureta and Arkhipkin 2007), and C_{day}, E_{day}, N_{day} are respectively catch (numbers of squid), fishing effort (numbers of vessels), and abundance (numbers of squid) per day. The catchability coefficient q summarized the range of variation of all trawls taken by the fishing fleet in this season.

In its basic form (DeLury 1947) the depletion model assumes a closed population in a fixed area for the duration of the assessment. However, the assumption of a closed population is imperfectly met in the Falkland Islands fishery, where stock analyses have often shown that *D. gahi* groups arrive in successive waves after the start of the season (Roa-Ureta 2012, Winter and Arkhipkin 2015). Arrivals of successive groups are inferred from discontinuities in the catch data. Fishing on a single, closed cohort would be expected to yield gradually decreasing CPUE, but gradually increasing average individual sizes, as the squid grow. When instead these data change suddenly, or in contrast to expectation, the immigration of a new group to the population is indicated (Winter and Arkhipkin 2015).

In the event of a new group arrival, the depletion calculation must be modified to account for this influx. Modification is done using a simultaneous algorithm that adds new arrivals on top of the stock previously present, and posits a common catchability coefficient for the entire depletion time-series. If two depletions are included in the same model (i.e., the stock present from the start plus a new group arrival), then:

$$C_{day} = q \times E_{day} \times (N1_{day} + (N2_{day} \times i2|_0^1)) \times e^{-M/2} \quad \textbf{(2)}$$

where i2 is a dummy variable taking the values 0 or 1 if 'day' is before or after the start day of the second depletion. For more than two depletions, $N3_{day}$, i3, $N4_{day}$, i4, etc., would be included following the same pattern.

The season depletion likelihood function was calculated as the difference between actual catch numbers reported and catch numbers predicted from the model (Equation **2**), statistically corrected by a factor relating to the number of days of the depletion period (Roa-Ureta 2012):

$$\text{minimization} \rightarrow \ ((n\text{Days} - 2)/2) \times \log\left(\sum_{days}\left(\log(\text{predicted } C_{day}) - \log(\text{actual } C_{day})\right)^2\right) \quad \textbf{(3)}$$

The stock assessment was set in a Bayesian framework (Punt and Hilborn 1997), whereby results of the season depletion model are conditioned by prior information on the stock; in this case the information from the pre-season survey.

The likelihood function of prior information was calculated as the normal distribution of the difference between catchability derived from the survey abundance estimate ($_{prior}q$), and catchability derived from the season depletion model ($_{depletion}q$). Applying this difference requires both the survey and the season to be fishing the same stock with the same gear. Catchability, rather than abundance N, is used for calculating prior likelihood because catchability informs the entire season time series; whereas N from the survey only informs the first in-season depletion period – subsequent immigrations and depletions are independent of the abundance that was present during the survey. Thus, the prior likelihood function was:

$$\text{minimization} \rightarrow \ \frac{1}{\sqrt{2\pi \cdot SD_{prior\ q}{}^2}} \times \exp\left(-\frac{\left({}_{depletion}q - {}_{prior}q\right)^2}{2 \cdot SD_{prior\ q}{}^2}\right) \quad \textbf{(4)}$$

where the standard deviation of catchability prior ($SD_{prior\ q}$) was calculated from the Euclidean sum (Carlson 2014) of the survey prior estimate uncertainty, the variability in catches on the season start date, and the uncertainty in the natural mortality M estimate over the number of days mortality discounting (Appendix Equation **A5**).

Bayesian optimization of the depletion was calculated by jointly minimizing Equations **3** and **4**, using the Nelder-Mead algorithm in R programming package 'optimx' (Nash and Varadhan 2011). Relative weights in the joint optimization were assigned to Equations **3** and **4** as the converse of their coefficients of variation (CV), i.e., the CV of the prior became the weight of the depletion model and the CV of the depletion model became the weight of the prior. Calculations of the depletion CVs are described in Equations **A8-S** and **A8-N**. Because a complex model with multiple depletions may converge on a local minimum rather than global minimum, the optimization was stabilized by running a feed-back loop that set the q and N parameter outputs of the Bayesian joint optimization back into the in-season-only minimization (Equation **3**), re-calculated the in-season-only minimization, then re-calculated the Bayesian joint optimization, and continued this process until both the in-season minimization and the joint optimization remained unchanged.

With actual C_{day}, E_{day} and M being fixed parameters, the optimization of Equation **2** using Equations **3** and **4** produces estimates of q and N1, N2, …, etc. Numbers of squid on the final day (or any other day) of a time series are then calculated as the numbers N of the depletion start days discounted for natural mortality during the intervening period, and subtracting cumulative catch also discounted for natural mortality (CNMD). Taking for example a two-depletion period:

$$\begin{aligned} N_{final\ day} &= N1_{start\ day\ 1} \times e^{-M\ (final\ day - start\ day\ 1)} \\ &+ N2_{start\ day\ 2} \times e^{-M\ (final\ day - start\ day\ 2)} \\ &- CNMD_{final\ day}, \end{aligned} \quad \textbf{(5)}$$

$$CNMD_{day\ 1} = 0$$

$$CNMD_{day\ x} = CNMD_{day\ x-1} \times e^{-M} + C_{day\ x-1} \times e^{-M/2} \quad \textbf{(6)}$$

$N_{final\ day}$ is then multiplied by the average individual weight of squid on the final day to give biomass. Daily average individual weight is obtained from length / weight conversion of mantle lengths measured in-season by observers, and also derived from in-season commercial data as the proportion of product weight that vessels reported per market size category[d]. Observer mantle lengths are scientifically more accurate, but restricted to a partial sample of trawls. Commercially proportioned mantle lengths are relatively less accurate, but cover every trawl of the entire fishing fleet every day. Therefore, both sources of data are used (see Appendix – *Doryteuthis gahi* individual weights).

Distributions of the likelihood estimates from joint optimization (i.e., measures of their statistical uncertainty) were computed using a Markov Chain Monte Carlo (MCMC) (Gamerman and Lopes 2006), a method that is commonly employed for fisheries assessments (Magnusson et al. 2013). MCMC is an iterative process which generates random stepwise changes to the proposed outcome of a model (in this case, the q and N of *D. gahi* squid) and at each step, accepts or nullifies the change with a probability equivalent to how well the change fits the model parameters compared to the previous step. The resulting sequence of accepted or nullified changes (i.e., the 'chain') approximates the likelihood distribution of the model

[d] First reported for Falkland Islands *D. gahi* by Payá (2006). Also used in some finfish commercial fisheries, see Plet-Hansen et al. 2018.

outcome. The MCMC of the depletion models were run for 200,000 iterations; the first 1000 iterations were discarded as burn-in sections (initial phases over which the algorithm stabilizes); and the chains were thinned by a factor equivalent to the maximum of either 5 or the inverse of the acceptance rate (e.g., if the acceptance rate was 12.5%, then every eighth (0.125^{-1}) iteration was retained) to reduce serial correlation. For each model three chains were run; one chain initiated with the parameter values obtained from the joint optimization of Equations **3** and **4**, one chain initiated with these parameters ×2, and one chain initiated with these parameters ×¼. Convergence of the three chains was accepted if the variance among chains was less than 10% higher than the variance within chains (Brooks and Gelman 1998). When convergence was satisfied the three chains were combined as one final set. Equations **5**, **6**, and the multiplication by average individual weight were applied to the CNMD and to each iteration of N values in the final set, and the biomass outcomes from these calculations represent the distribution of the estimate.

Depletion models and likelihood distributions were calculated separately for north and south sub-areas of the Loligo Box fishing zone, as *D. gahi* sub-stocks emigrate from different spawning grounds and remain to an extent segregated (Arkhipkin and Middleton 2002). However, q_{prior} was calculated for the north and south sub-areas combined, rather than separately (Equation **A4**). As fishing tends to start predominantly in one or the other sub-area, rather than the fleet spreading itself evenly, separately computed north and south qs_{prior} are susceptible to arbitrary differences. Total escapement biomass was then defined as the aggregate biomass of *D. gahi* on the last day of the season for north and south sub-areas combined. North and south biomasses are not assumed to be uncorrelated however (Shaw et al. 2004), and therefore north and south likelihood distributions were added semi-randomly in proportion to the strength of their day-to-day correlation (see Winter 2014, for the semi-randomization algorithm).

Stock assessment

Catch and effort

The north sub-area was fished on 57 of 68 season-days, for 56.9% of total catch (32074.7 t *D. gahi*) and 56.8% of effort (548.7 vessel-days) (Figures 2 and 3). The south sub-area was fished on 49 of the 68 season-days, for 43.1% of total catch (24342.3 t *D. gahi*) and 43.2% of effort (417.3 vessel-days); demonstrating near-equal CPUE north and south. The proportion of catch north was the highest for a first season since 2018, which was also partially driven by closures in the south (Winter 2018).

Data

966 vessel-days were fished during the season (Table 1), with a median of 15 vessels per day (mean 14.21). Vessels reported daily catch totals to the FIFD and electronic logbook data that included trawl times, positions, depths, and product weight by market size categories. Three FIG fishery observers were deployed on four vessels in the fishing season for a total of 54 sampling days[e] (Copping 2022, Nicholls 2022a, b, Sadd 2022). Throughout the 68 days of the season, 20 days had no FIG fishery observer sampling, 42 days had 1 FIG fishery observer sampling, and 6 days had two FIG fishery observers sampling. Except for seabird days FIG fishery observers were tasked with sampling 200 *D. gahi* at two stations daily; reporting their

[e] Not counting seabird days (every fourth day).

maturity stages, sex, and lengths to 0.5 cm. Contract marine mammal observers were tasked with measuring 200 unsexed lengths of *D. gahi* per day. The length-weight relationship for converting observer and commercially proportioned lengths was combined from first pre-season and season length-weight data of both 2021 and 2022, as 2022 data became available progressively with on-going observer coverage. The final parameterization of the length-weight relationship included 4390 measures from 2021 and 5821 measures from 2022, giving:

$$\text{weight (kg)} = 0.16011 \times \text{length (cm)}^{2.23805} / 1000 \quad \textbf{(7)}$$

with a coefficient of determination $R^2 = 93.0\%$.

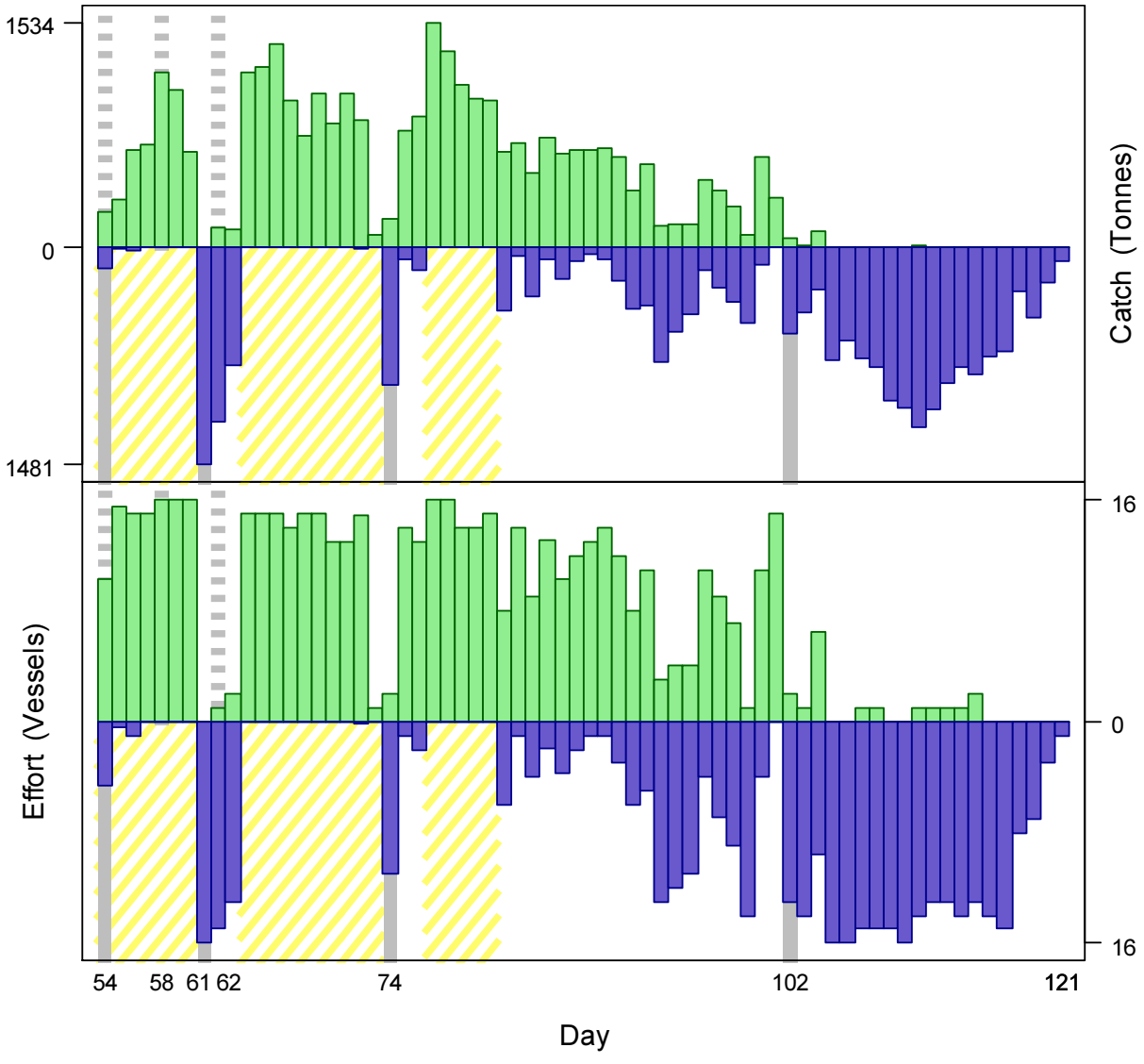

Figure 3. Daily total *D. gahi* catch and effort distribution by assessment sub-area north (green) and south (purple) of the 52° S parallel during 1st season 2022. The season was open from February 23rd (chronological day 54) with directed closure scheduled on April 27th (day 117), and flex days until May 1st (day 121). Yellow shading: temporary exclusion of the sub-area south of 52.5 °S. As many as 16 vessels fished per day north; as many as 16 vessels fished per day south. As much as 1534 tonnes *D. gahi* was caught per day north; as much as 1481 tonnes *D. gahi* was caught per day south.

Group arrivals / depletion criteria

Start days of depletions - following arrivals of new *D. gahi* groups - were judged primarily by daily changes in CPUE, with additional information from sex proportions, maturity, and average individual squid sizes. CPUE was calculated as metric tonnes of *D. gahi* caught per vessel per day. Days were used rather than trawl hours as the basic unit of effort. Commercial vessels do not trawl standardized duration hours, but rather durations that best suit their daily processing requirements. An effort index of days is therefore more consistent (FIFD 2004, Winter and Arkhipkin 2015). Inclusion of additional depletion starts was partially evaluated by improvement of the Akaike information criterion (Akaike 1973) on model fit. However, when the model is used for in-season monitoring, a new depletion start will almost certainly give a poorer AIC until a number of days have passed for better fit to supersede the penalty of the additional parameter. Improvement was therefore defined as showing a trend towards relatively lower AIC over progressive days rather than necessarily an outright lower AIC, so that depletion starts could be included as soon as their relevance was evident, and align the in-season model as soon as possible with the final post-season model.

Four days south and three days north were ultimately identified that represented the onset of significant immigrations / depletions throughout the season. A fourth immigration peak in the north was evaluated, but did not meet criteria for substantiated influence on the depletion model. The last days of fishing in the south had high CPUE peaks, but were considered 'fill-up' catches by the few remaining vessels and not a further immigration event.

- The first depletion start south was set by definition on day 54 (February 23rd), the first day of the season with five vessels fishing south. Individual weights and maturities on that day were average for the season (Figure 4A, 4B, 4D); CPUE was low (Figure 5).
- The second depletion start south was identified on day 61 (March 2nd), as the south was re-opened to fishing. CPUE was the highest in the south for the season (Figure 5). Average individual commercial weight was lower than previously (Figure 4A). The proportion of females was the highest south all season and decreased over the next two days (Figure 4C). Average maturities were lower than previously and increased over the next two days (Figure 4D).
- The third depletion start south was identified on day 74 (March 15th), again as the south was re-opened to fishing. CPUE was highest since the previous depletion start and slightly higher again the day after, but for the subsequent period fishing effort remained low in the south (Figure 5).
- The fourth depletion start south was identified on day 109 (April 19th). Average weights, female proportion, and average maturities all showed dips or relatively low values that day (Figure 4). CPUE was on an increasing trend (Figure 5) which suggested a period of diffuse, rather than sudden, immigration.
- The first depletion start north was set by definition on day 54 (February 23rd), the first day of the season with eleven vessels fishing north. CPUE was still low (Figure 5), average individual weights were low (Figure 4A, 4B), but the proportion of females was the highest of the season north (Figure 4C).
- The second depletion start north was identified on day 58 (February 27th), with a strong peak in CPUE (Figure 5). Average individual weights (Figure 4A, 4B) and average maturities (Figure 4D) were relatively high that day, suggesting the possibility that this day represented a concentration more than a true immigration.
- The third depletion start north was identified on day 62 (March 3rd) with the highest CPUE of the season (albeit fished by only one vessel). CPUEs were lower but still consistently high over the following days (Figure 5).

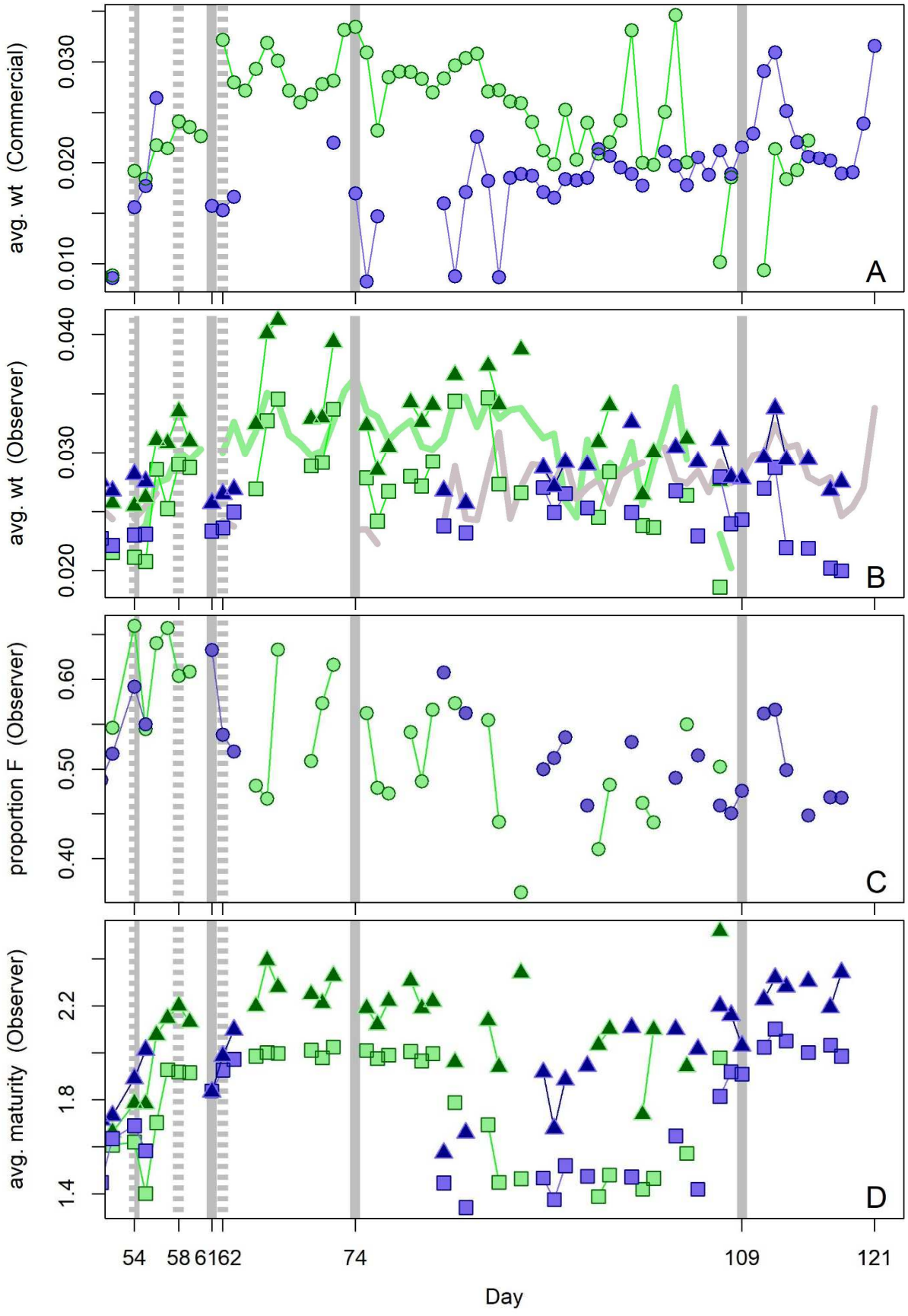
avg. wt (Commercial)
0.010
0.020
0.030
A
avg. wt (Observer)
0.020
0.030
0.040
B
proportion F (Observer)
0.40
0.50
0.60
C
avg. maturity (Observer)
1.4
1.8
2.2
D
54
58
61
62
74
109
121
Day

Figure 4 [previous page]. A: Average individual *D. gahi* weights (kg) per day from commercial size categories. B: Average individual *D. gahi* weights (kg) by sex per day from FIG observer sampling. C: Proportions of female *D. gahi* per day from observer sampling. D: Average maturity index value (Lipiński 1979) by sex per day from observer sampling. Males: triangles, females: squares, combined: circles. Thick lines (B) are unsexed measurements from the contract marine mammal observers. North sub-area: green, south sub-area: purple. Data from consecutive days are joined by line segments. Broken grey bars: starts of in-season depletions north. Solid grey bars: starts of in-season depletions south.

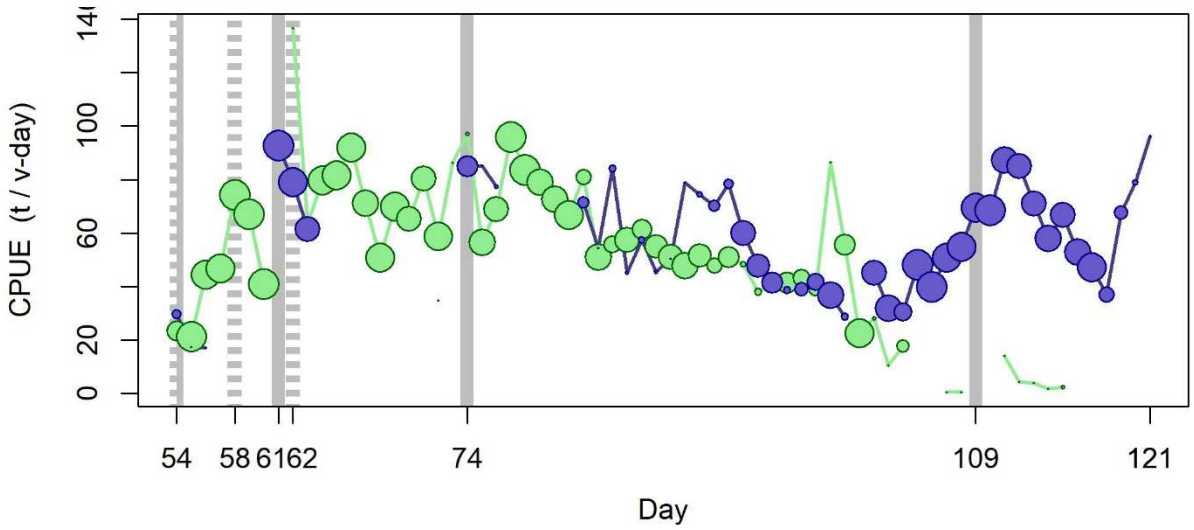

Figure 5. CPUE in metric tonnes per vessel per day, by assessment sub-area north (green) and south (purple) of 52° S latitude. Circle sizes are proportioned to numbers of vessels fishing. Data from consecutive days are joined by line segments. Broken grey bars indicate the starts of in-season depletions north. Solid grey bars indicate the starts of in-season depletions south.

Depletion analyses

South

In the south sub-area, the maximum likelihood posterior ($_{\text{Bayesian}}\, q_S = 0.623 \times 10^{-3}$; Figure 6-left, and Equation **A9-S**) was preponderantly optimized on the prior ($_{\text{prior}}\, q = 0.566 \times 10^{-3}$; Figure 6-left, and Equation **A4**); even though in-season depletion ($_{\text{depletion}}\, q_S = 1.736 \times 10^{-3}$; Figure 6-left, and **A6-S**) had 3× higher weight than the prior in the Bayesian model (Equations **A5** and **A8-S**). Modelling of the south sub-area had a generally poor outcome, concordant with the repeated interruptions of fishing effort.

The MCMC distribution of the Bayesian posterior multiplied by the GAM fit of average individual squid weight (Figure A1-south) gave the likelihood distribution of *D. gahi* biomass on day 121 (May 1st) shown in Figure 6-right, with maximum likelihood and 95% confidence interval of:

$$B_{S\ \text{day}\ 121} = 83{,}415\ \text{t} \sim 95\%\ \text{CI}\ [69{,}526 – 292{,}789]\ \text{t} \qquad \textbf{(8-S)}$$

On the first day of the season estimated *D. gahi* biomass south was 33,655 t ~ 95% CI [26,447 – 120,703] t (Figure 7); not statistically different from the pre-season estimate of 29,894 t [27,650 – 41,788] (Winter et al. 2022). The highest biomass estimate of the season occurred with the fourth immigration on day 109, reaching 124,769 t [95,463 – 401,872]. Effectively,

the variation of biomass estimate throughout the season was not statistically significant; by the rule that a straight line could be drawn through the plot (Figure 7) without intersecting the 95% confidence interval (Swartzman et al. 1992).

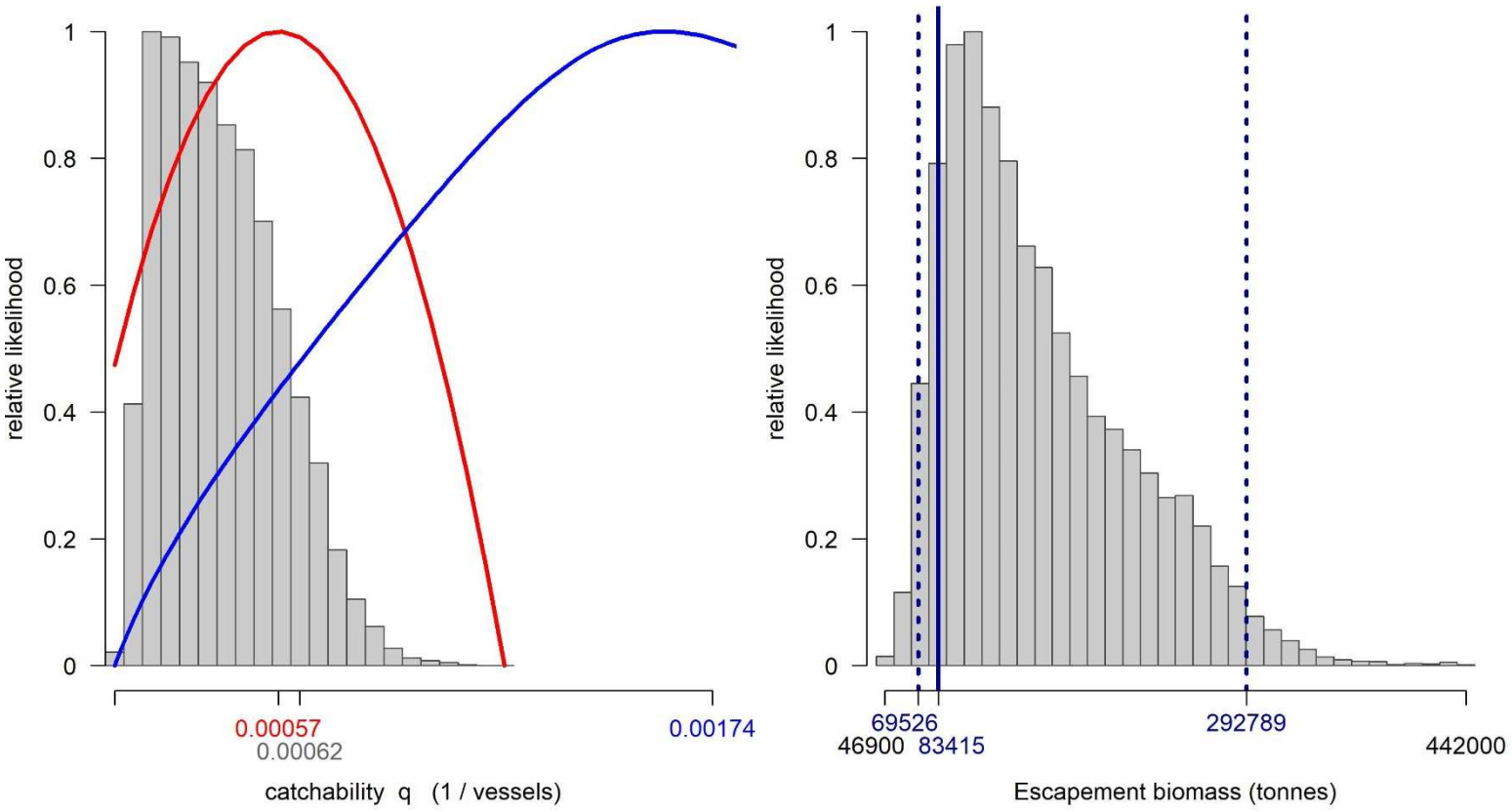

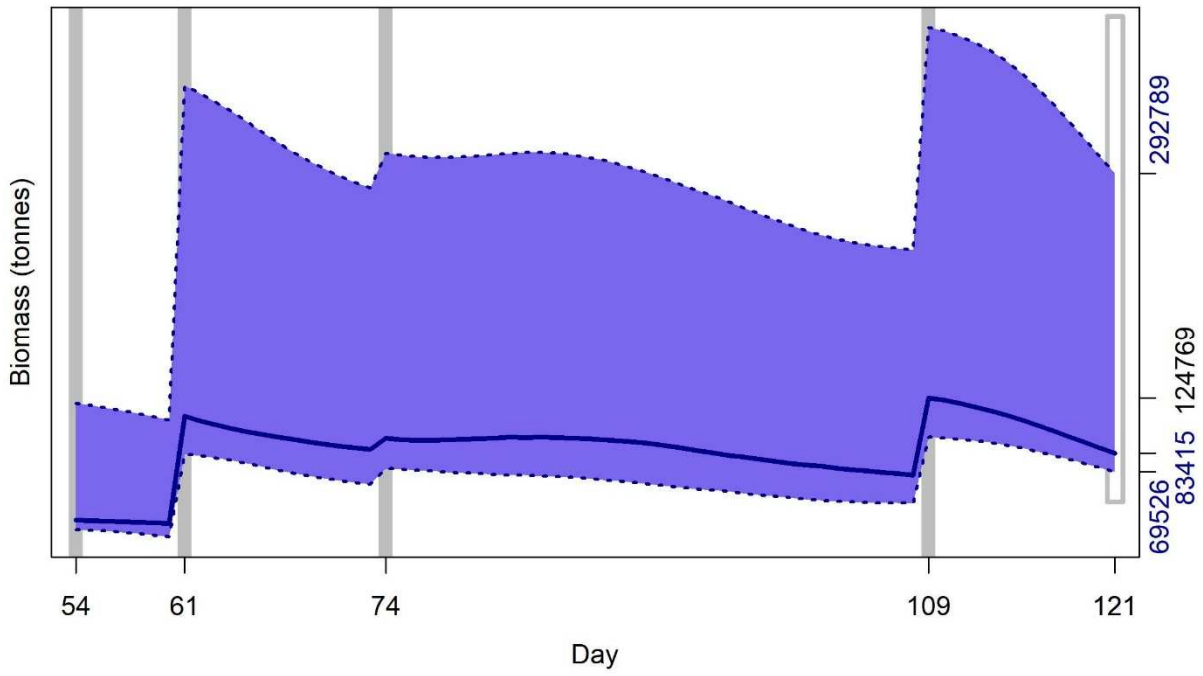

Figure 6 [previous page – top]. South sub-area. Left: Likelihood distributions for *D. gahi* catchability. Red line: prior model (pre-season survey data), blue line: in-season depletion model, grey bars: combined Bayesian model posterior. Right: Likelihood distribution (grey bars) of escapement biomass, from Bayesian posterior and average individual squid weight at the end of the season. Blue lines: maximum likelihood and 95% confidence interval. Note correspondence to Figure 7.

Figure 7 [previous page – bottom]. South sub-area. *D. gahi* biomass time series estimated from Bayesian posterior of the depletion model ± 95% confidence interval. Grey bars indicate the start of in-season depletions south; days 54, 61, 74 and 109. Note that the biomass 'footprint' on day 121 (May 1st) corresponds to the right-side plot of Figure 6.

North

In the north sub-area, the maximum likelihood posterior ($_{\text{Bayesian}}\, q_N = 0.630 \times 10^{-3}$; Figure 8-left, and Equation **A9-N**) was preponderantly optimized on the prior ($_{\text{prior}}\, q = 0.566 \times 10^{-3}$; Figure 8-left, and Equation **A4**). The in-season depletion ($_{\text{depletion}}\, q_N = 3.957 \times 10^{-3}$; off the scale on Figure 8-left, and Equation **A6-N**) had higher weight (lower CV) than the prior in the Bayesian model (Equations **A5** and **A8-N**), but with most of the season being a single continuous slope (Figure 9), its parameters were relatively non-selective.

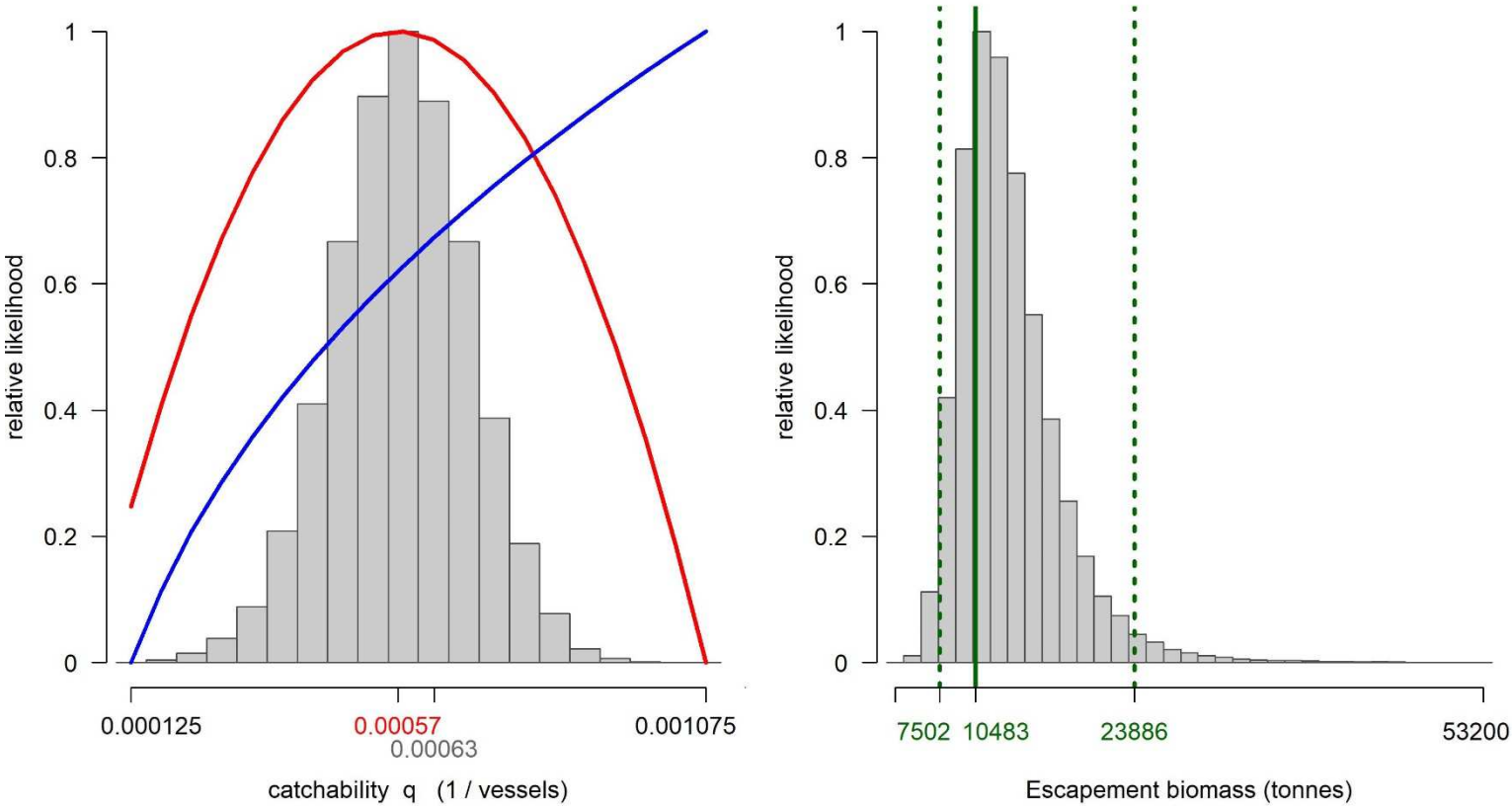

Figure 8. North sub-area. Left: Likelihood distributions for *D. gahi* catchability. Red line: prior model (pre-season survey data), blue line: in-season depletion model, grey bars: combined Bayesian model posterior. Right: Likelihood distribution (grey bars) of escapement biomass, from Bayesian posterior and average individual squid weight at the end of the season. Green lines: maximum likelihood and 95% confidence interval. Note the correspondence to Figure 9.

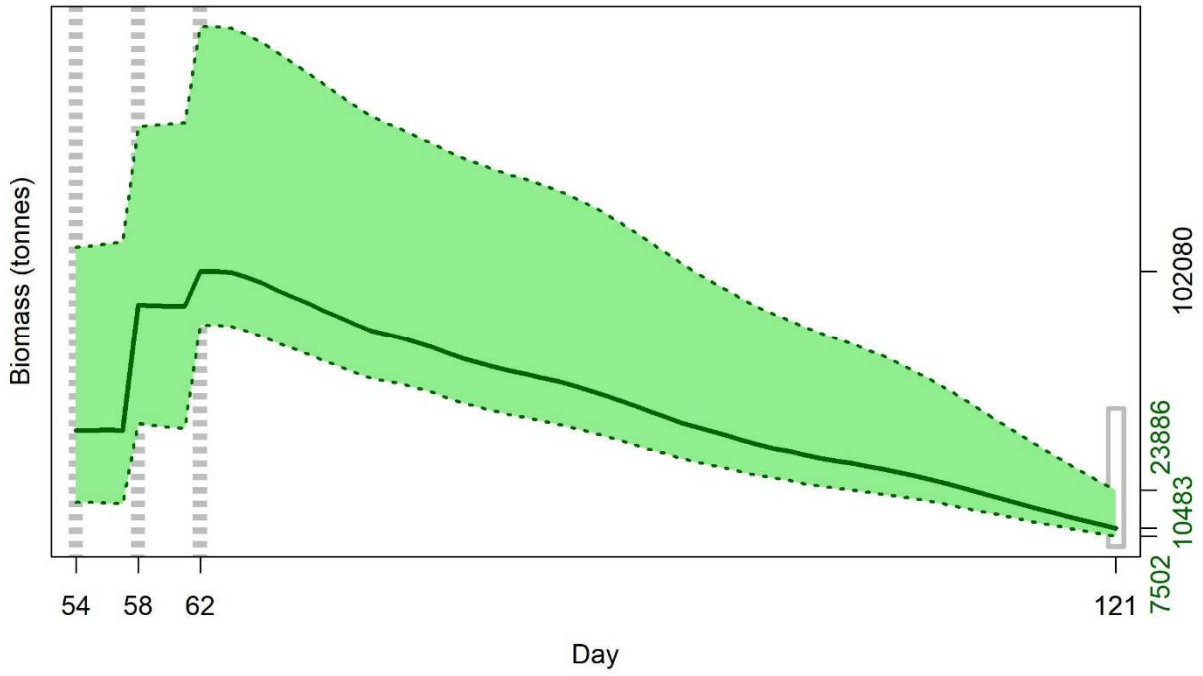

Figure 9. North sub-area. *D. gahi* biomass time series estimated from Bayesian posterior of the depletion model ± 95% confidence interval. Broken grey bars indicate the start of in-season depletions north; days 54, 58 and 62. Note that the biomass 'footprint' on day 121 (May 1st) corresponds to the right-side plot of Figure 8.

The MCMC distribution plus average individual weight variation gave the likelihood distribution of *D. gahi* biomass on day 121 (May 1st) shown in Figure 8-right, with maximum likelihood and 95% confidence interval of:

$$B_{N\ day\ 121} = 10{,}483\ t \sim 95\%\ CI\ [7{,}502 – 23{,}886]\ t \quad \textbf{(8-N)}$$

On the first day of the season estimated *D. gahi* biomass north was 45,141 t ~ 95% CI [19,686 – 110,549] t, significantly higher than the pre-season estimate of 17,165 t [8,839 – 22,205] (Winter et al. 2022). The highest biomass estimate of the season occurred with the second immigration on day 62, reaching 102,080 t [82,710 – 189,177]. Biomass then decreased continuously until the final day (Figure 9).

Immigration

Doryteuthis gahi immigration during the season was inferred on each day by how many more squid were estimated present than the day before, minus the number caught and the number expected to have died naturally:

$$_{Immigration}N_{day\ i} = N_{day\ i} – (N_{day\ i-1} – C_{day\ i-1} – M_{day\ i-1})$$

where $N_{day\ i-1}$ are optimized in the depletion models, $C_{day\ i-1}$ calculated as in Equations **2** and **3**, and $M_{day\ i-1}$ is:

$$M_{\text{day i-1}} = (N_{\text{day i-1}} - C_{\text{day i-1}}) \times (1 - e^{-M})$$

Immigration biomass per day was then calculated as the immigration number per day multiplied by predicted average individual weight from the GAM:

$$_{\text{Immigration}}B_{\text{day i}} = {}_{\text{Immigration}}N_{\text{day i}} \times {}_{\text{GAM}}Wt_{\text{day i}}$$

All numbers N are themselves derived from the daily average individual weights, therefore the estimation automatically factors in that those squid immigrating on a given day would likely be smaller than average (because younger). Confidence intervals of the immigration estimates were calculated by applying the above algorithms to the MCMC iterations of the depletion models. Resulting total biomasses of *D. gahi* immigration north and south, up to season end (day 121), were:

$$_{\text{Immigration}}B_{\text{S season}} = 147{,}798 \text{ t} \sim 95\% \text{ CI } [122{,}190 \text{ to } 453{,}271] \text{ t} \quad \textbf{(9-S)}$$

$$_{\text{Immigration}}B_{\text{N season}} = 48{,}056 \text{ t} \sim 95\% \text{ CI } [10{,}419 \text{ to } 115{,}723] \text{ t} \quad \textbf{(9-N)}$$

Total immigration with semi-randomized addition of the confidence intervals was:

$$_{\text{Immigration}}B_{\text{Total season}} = 195{,}855 \text{ t} \sim 95\% \text{ CI } [163{,}981 \text{ to } 519{,}171] \text{ t} \quad \textbf{(9-T)}$$

In the south sub-area, the in-season peaks on days 61, 74, and 109 accounted for approximately 53.6%, 6.0%, and 39.1% of in-season immigration (start day 54 was de facto not an in-season immigration); suggesting that the day 74 peak may have been mostly a re-concentration of squid following the pause in fishing. In the north sub-area, the in-season peaks on days 58 and 62 accounted for approximately 77.8% and 21.1% of in-season immigration. Both south and north, the remaining immigration percentages were accounted for by the minor fluctuations throughout the season.

Escapement biomass

Total escapement biomass was defined as the aggregate biomass of *D. gahi* at the end of day 121 (May 1st) for south and north sub-areas combined (Equations **9**). Depletion models are calculated on the inference that all fishing and natural mortality are gathered at mid-day, thus a half day of mortality ($e^{-M/2}$) was added to correspond to the closure of the fishery at 23:59 (mid-night) on May 1st for the final remaining vessels: Equation **10**.

$$B_{\text{Total day 276}} = (B_{\text{S day 121}} + B_{\text{N day 121}}) \times e^{-M/2}$$

$$= 93{,}898 \text{ t} \times 0.99336$$

$$= 93{,}275 \text{ t} \sim 95\% \text{ CI } [81{,}579 - 304{,}984] \text{ t} \quad \textbf{(10)}$$

South and north biomass time series were effectively uncorrelated at $R = -0.0402$). Semi-randomized addition of the south and north distributions gave the aggregate likelihood of total escapement biomass ($B_{\text{Total day 121}}$) shown in Figure 10. The estimated escapement biomass of 93,275 t was the highest on record since at least 2004. The risk of the fishery in the current season, defined as the proportion of the total escapement biomass distribution below

the conservation limit of 10,000 tonnes (Agnew et al. 2002, Barton 2002), was effectively zero. For comparison, the minimum aggregate biomass of the season was estimated on day 57 (February 26th) as 77,448 t ~ 95% CI [56,805 – 190,118] t; also with zero risk of < 10,000 tonnes.

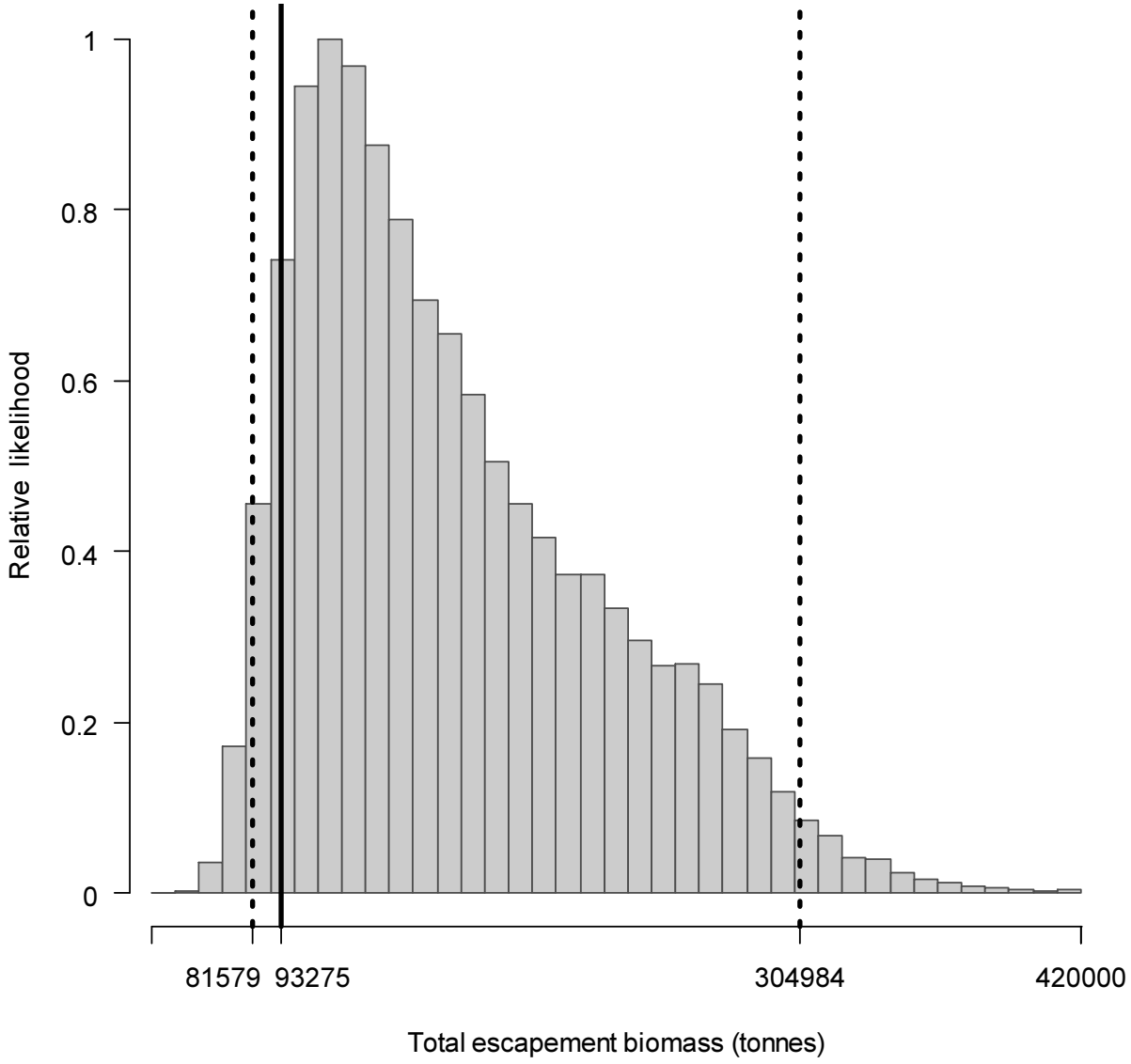

Figure 10. Likelihood distribution with 95% confidence interval of total *D. gahi* escapement biomass at the season end (May 1st).

Fishery bycatch

All except three of the 966 first season vessel-days (Table 1) reported *D. gahi* squid as their primary catch. The exceptions were three relatively small catch reports in the north sub-area in mid- to late-April, that reported 0.654, 0.439 and 0.708 common hake (*Merluccius hubbsi*) vs. 0.198, 0.415 and 0.272 *D. gahi*. The proportion of season total catch represented by *D. gahi* (56417038/57753091 = 0.977; Table A1) is the lowest for a first season since 2018 (a year of high medusae; Winter 2018).

Figure 11 [below]. Distributions of the six main bycatches during first season 2022, by noon position grids. Thickness of grid lines is proportional to the number of vessel-days (1 to 186 per grid; 21 different grids were occupied). Grey-scale is proportional to the bycatch biomass; maximum (tonnes) indicated on each plot.

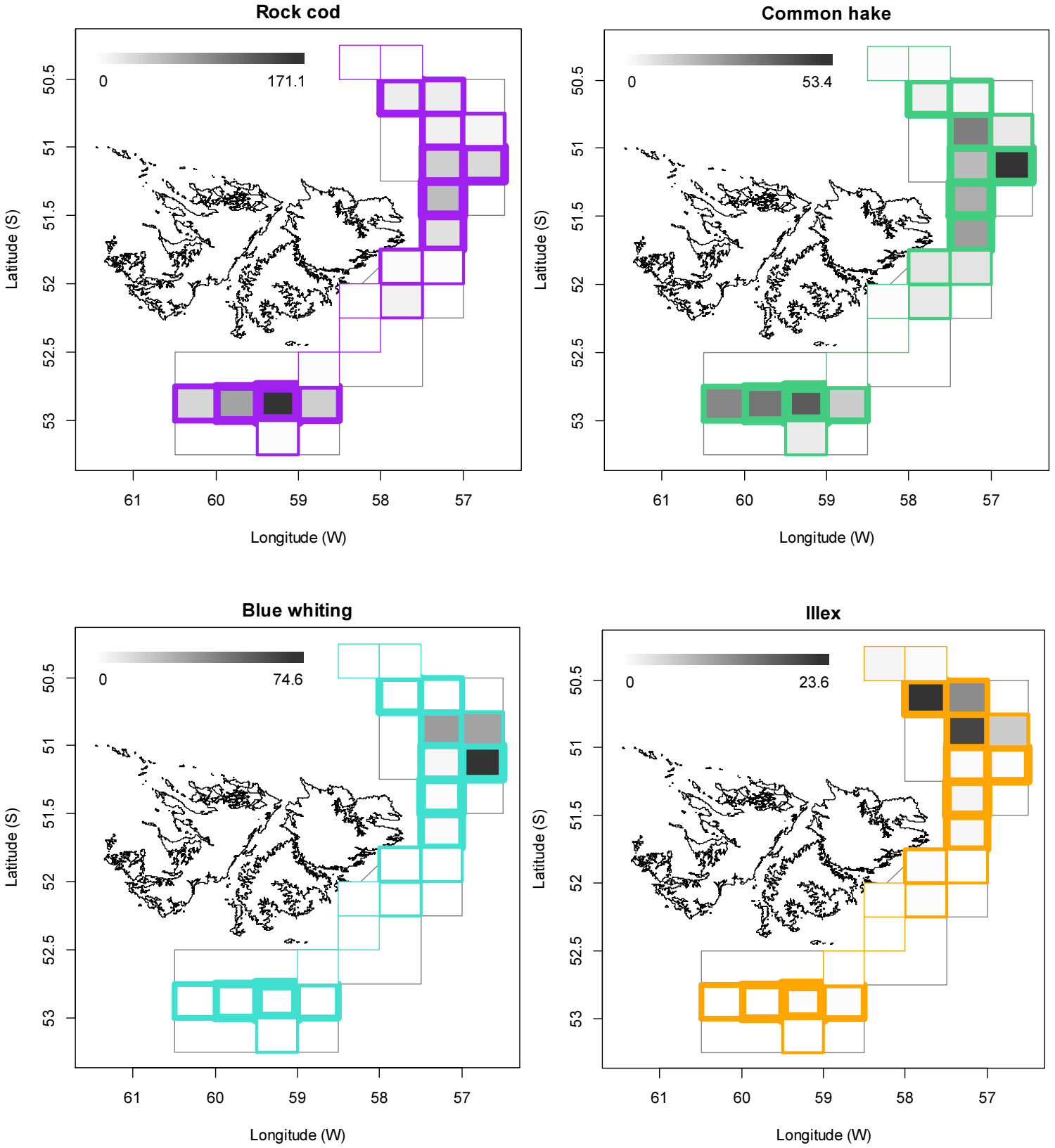

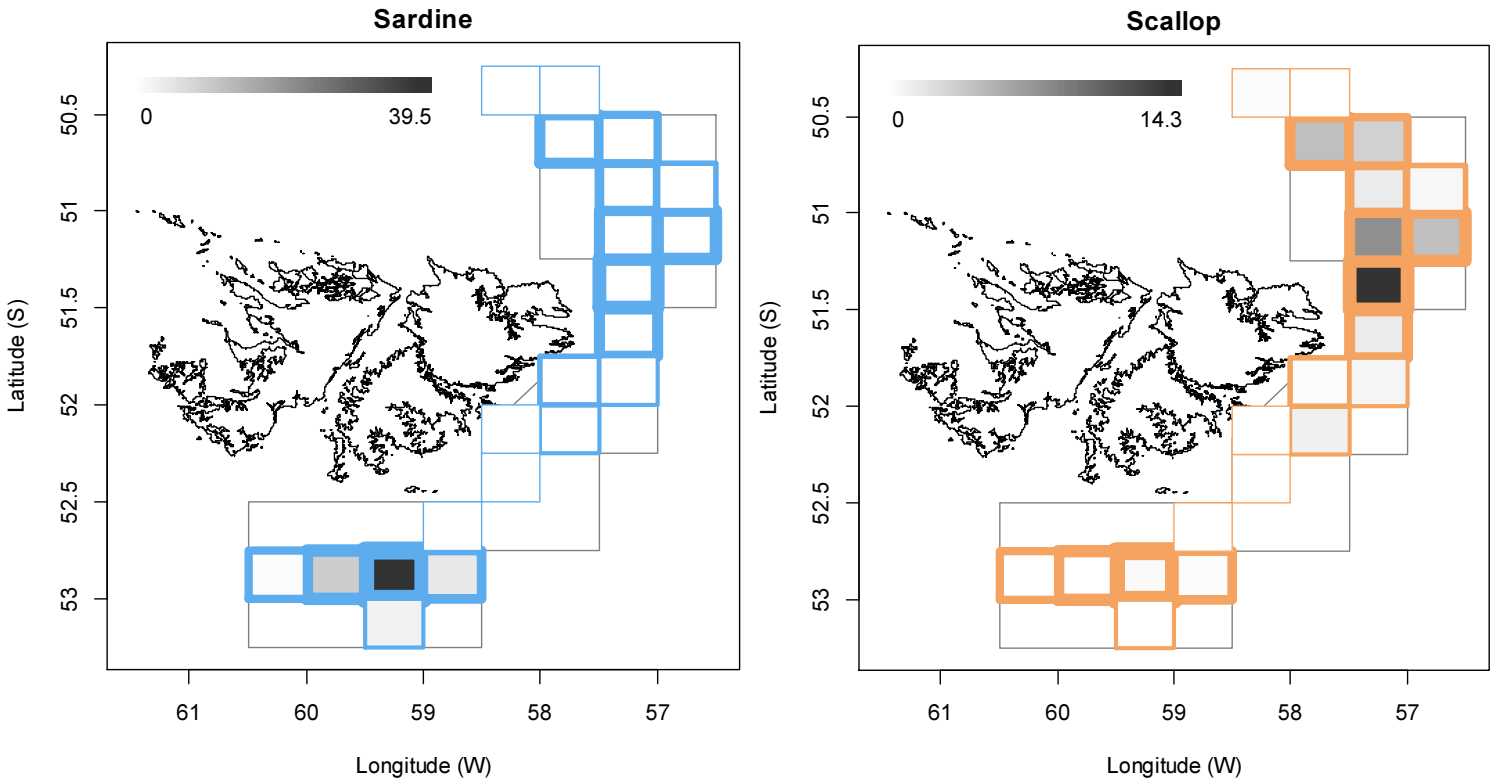

Highest aggregate bycatches in first season 2022 were common rock cod *Patagonotothen ramsayi* with 556 tonnes from 965 vessel-days (catch reports), common hake *Merluccius hubbsi* (316 t, 608 v-days), southern blue whiting *Micromesistius australis australis* (149 t, 73 v-days), shortfin squid *Illex argentinus* (71 t, 387 v-days), sardine *Sprattus fuegensis* (57 t, 126 v-days), and scallops probably *Zygochlamys* (40 t, 413 v-days). Relative distributions by grid of these bycatches are shown in Figure 11; the complete list of all catches by species is in Table A1.

Other than *D. gahi* itself, the most concentrated catch was southern blue whiting with 149445 kg in 73 vessel-days (= 2047.2 kg/vessel-day; Table A1). Of that amount, 99% were taken in just 49 vessel-days (= 3021.3 kg/vessel-day). Eight catch reports had southern blue whiting exceeding the 10% bycatch threshold, all in grids XMAP, XMAQ, or XNAQ (Figure 11 – Blue whiting), in early April[f]. One of these eight catch reports listed most of its southern blue whiting commercially retained. Localized high clusters of southern blue whiting in the *D. gahi* fishing zone are not uncommon (e.g., Winter and Juergens 2014), but this season had the highest first season total southern blue whiting catch since 2002 (= 284206 kg); a time when southern blue whiting catches and abundance were generally higher (Ramos and Winter 2021).

Trawl area coverage

The impact of bottom trawling on seafloor habitat has been a matter of concern in commercial fisheries (Kaiser et al. 2002; 2006), whereby the potential severity of impact relates to spatial and temporal extents of trawling (Piet and Hintzen 2012, Gerritsen et al. 2013), as well as the type of trawl gear (Rijnsdorp et al. 2020). For the *D. gahi* fishery, available catch, effort, and

[f] Management action was not taken, as vessels moved voluntarily and the incidence did not recur.

positional data are used to summarize the estimated 'ground' area coverage[g] occupied during the season of trawling.

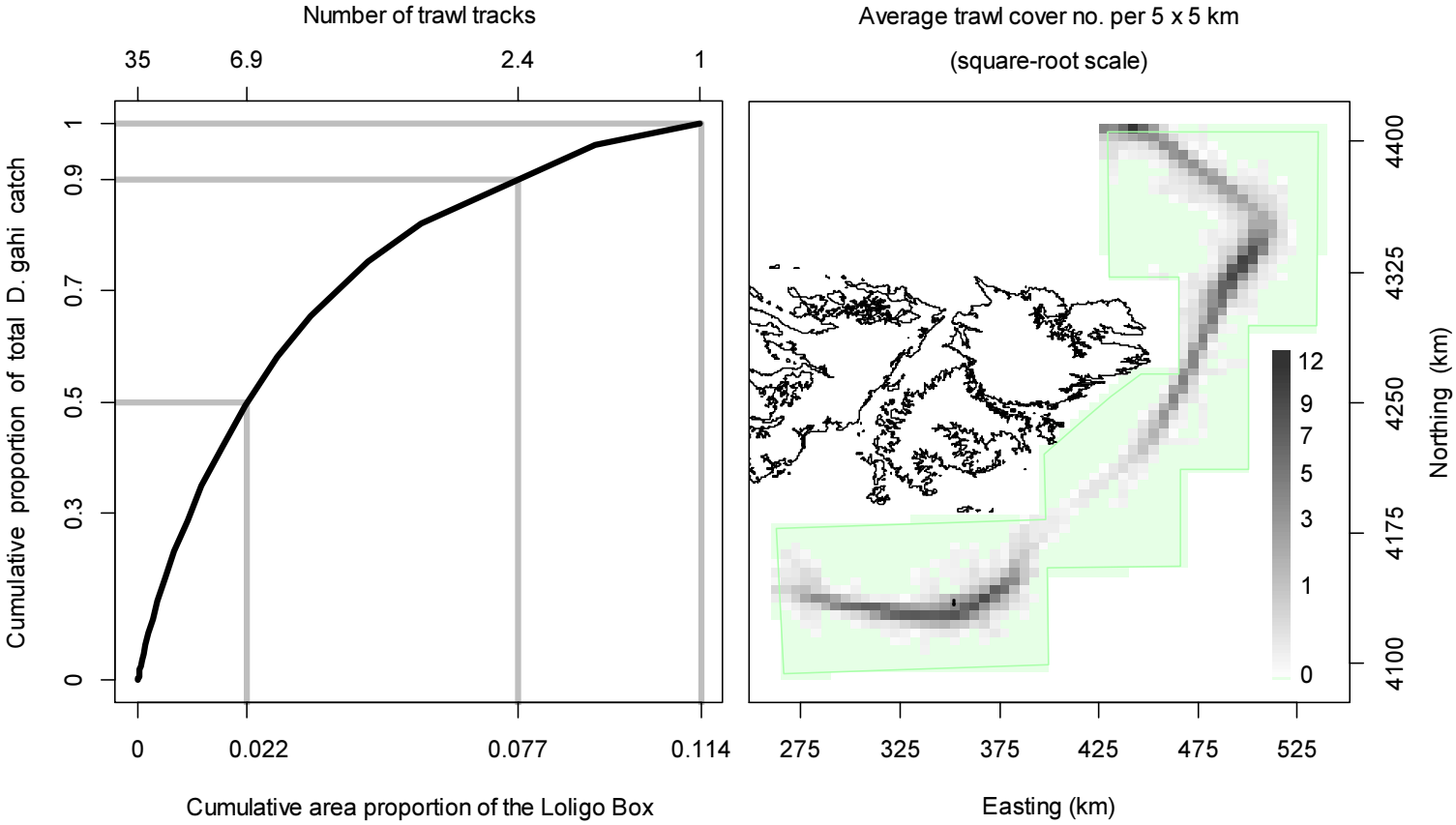

Figure 12. Left: cumulative *D. gahi* catch of 1st season 2022, vs. cumulative area proportion of the Loligo Box the catch was taken from. The maximum number of times that any single area unit was trawled was 35, and catch cumulation by reverse density corresponded approximately to the trawl multiples shown on the top x-axis. Right: trawl cover averaged by 5 × 5 km grid; green area represents zero trawling.

The procedure for summarizing trawl area coverage is described in the Appendix of the second season 2019 report (Winter 2019). In first season 2022 50% of total *D. gahi* catch was taken from 2.2% of the total area of the Loligo Box, corresponding approximately[h] to the aggregate of grounds trawled ≥6.9 times. 90% of total *D. gahi* catch was taken from 7.7% of the total area of the Loligo Box, corresponding approximately to the aggregate of grounds trawled ≥2.4 times. 100% of total *D. gahi* catch over the season was taken from 11.4% of the total area of the Loligo Box, obviously corresponding to the aggregate of all grounds trawled at least once (Figure 12 - left). The 11.4% total trawl area coverage is median among the eight seasons that have been given this analysis so far. Averaged by 5 × 5 km grid (Figure 12 - right), 2 grids (out of 1383) had coverage of 10 or more (that is to say, every patch of ground within

[g] Appropriate spatial scale for calculating area coverage is a matter of some debate (Amoroso et al. 2018, Kroodsma et al. 2018). Given the comparatively small area of the Loligo Box, a high resolution of 5 km × 5 km was used for these calculations.

[h] However, not exactly. There is an expected strong correlation between the density of *D. gahi* catch taken from area units and how often these area units were trawled, but the correlation is not perfectly monotonic.

that 5 × 5 km was on average trawled over 10 times or more). Thirty-four grids had coverage of 5 or more, and 108 grids had coverage of 2 or more.

References

Agnew, D.J., Baranowski, R., Beddington, J.R., des Clers, S., Nolan, C.P. 1998. Approaches to assessing stocks of *Loligo gahi* around the Falkland Islands. Fisheries Research 35: 155-169.

Agnew, D. J., Beddington, J. R., and Hill, S. 2002. The potential use of environmental information to manage squid stocks. Canadian Journal of Fisheries and Aquatic Sciences, 59: 1851–1857.

Akaike, H. 1973. Information theory and an extension of the maximum likelihood principle. 2nd International Symposium on Information Theory: 267-281.

Amoroso, R.O., Parma, A.M., Pitcher, C.R., McConnaughey, R.A., Jennings, S. 2018. Comment on "Tracking the global footprint of fisheries". Science 361: eaat6713.

Arkhipkin, A. 1993. Statolith microstructure and maximum age of *Loligo gahi* (Myopsida: Loliginidae) on the Patagonian Shelf. Journal of the Marine Biological Association of the UK 73: 979-982.

Arkhipkin, A.I., Middleton, D.A.J. 2002. Sexual segregation in ontogenetic migrations by the squid *Loligo gahi* around the Falkland Islands. Bulletin of Marine Science 71: 109-127.

Arkhipkin, A.I., Middleton, D.A.J., Barton, J. 2008. Management and conservation of a short-lived fishery resource: *Loligo gahi* around the Falkland Islands. American Fisheries Society Symposium 49: 1243-1252.

Arkhipkin, A.I., Hendrickson, L.C., Payá, I., Pierce, G.J., Roa-Ureta, R.H., Robin, J.-P., Winter, A. 2021. Stock assessment and management of cephalopods: advances and challenges for short-lived fishery resources. ICES Journal of Marine Science 78: 714-730.

Barton, J. 2002. Fisheries and fisheries management in Falkland Islands Conservation Zones. Aquatic Conservation: Marine and Freshwater Ecosystems 12: 127–135.

Brooks, S.P., Gelman, A. 1998. General methods for monitoring convergence of iterative simulations. Journal of computational and graphical statistics 7:434-455.

Carlson, J.E. 2014. A generalization of Pythagoras's theorem and application to explanations of variance contributions in linear models. Research Report No. RR-14-18, Princeton, NJ: Educational Testing Service. 17 p.

Copping, L. 2022. Observer Report 1326. Technical Document, FIG Fisheries Department. 23 p.

DeLury, D.B. 1947. On the estimation of biological populations. Biometrics 3: 145-167.

FIFD. 2004. Fishery Report, *Loligo gahi*, Second Season 2004. Fishing statistics, biological trends, and stock assessment. Technical Document, Falkland Islands Fisheries Department. 15 p.

Gamerman, D., Lopes, H.F. 2006. Markov Chain Monte Carlo. Stochastic simulation for Bayesian inference. 2nd edition. Chapman & Hall/CRC.

Gerritsen, H.D., Minto, C., Lordan, C. 2013. How much of the seabed is impacted by mobile fishing gear? Absolute estimates from Vessel Monitoring System (VMS) point data. ICES Journal of Marine Science 70: 523-531.

Hoenig, J.M. 1983. Empirical use of longevity data to estimate mortality rates. Fishery Bulletin 82: 898-903

Kaiser, M.J., Collie, J.S., Hall, S.J., Jennings, S., Poiner, I.R. 2002. Modification of marine habitats by trawling activities: prognosis and solutions. Fish and Fisheries 3: 114-136.

Kaiser, M.J., Clarke, K.R., Hinz, H., Austen, M.C.V., Somerfield, P.J., Karakassis, I. 2006. Global analysis of response and recovery of benthic biota to fishing. Marine Ecology Progress Series 311: 1-14.

Kroodsma, D.A., Mayorga, J., Hochberg, T., Miller, N.A., Boerder, K., Ferretti, F., Wilson, A., Bergman, B., White, T.D., Block, B.A., Woods, P., Sullivan, B., Costello, C., Worm, B. 2018. Response to Comment on "Tracking the global footprint of fisheries". Science 361: eaat7789.

Lipiński, M. R. 1979. Universal maturity scale for the commercially important squids (Cephalopoda: Teuthoidea). The results of maturity classification of *Illex illecebrosus* (Le Sueur 1821) population for years 1973–1977. ICNAF Research Document 79/11/38, 40 p.

Magnusson, A., Punt, A., Hilborn, R. 2013. Measuring uncertainty in fisheries stock assessment: the delta method, bootstrap, and MCMC. Fish and Fisheries 14: 325-342.

Nash, J.C., Varadhan, R. 2011. optimx: A replacement and extension of the optim() function. R package version 2011-2.27. http://CRAN.R-project.org/package=optimx

Nicholls, R. 2022a. Observer Report 1318. Technical Document, FIG Fisheries Department. 19 p.

Nicholls, R. 2022b. Observer Report 1323. Technical Document, FIG Fisheries Department. 29 p.

Patterson, K.R. 1988. Life history of Patagonian squid *Loligo gahi* and growth parameter estimates using least-squares fits to linear and von Bertalanffy models. Marine Ecology Progress Series 47: 65-74.

Payá, I. 2006. Fishery Report. *Loligo gahi*, Second Season 2006. Fishery statistics, biological trends, stock assessment and risk analysis. Technical Document, Falkland Islands Fisheries Dept. 40 p.

Payá, I. 2010. Fishery Report. *Loligo gahi*, Second Season 2009. Fishery statistics, biological trends, stock assessment and risk analysis. Technical Document, Falkland Islands Fisheries Dept. 54 p.

Pierce, G.J., Guerra, A. 1994. Stock assessment methods used for cephalopod fisheries. Fisheries Research 21: 255–285.

Piet, G.J., Hintzen, N.T. 2012. Indicators of fishing pressure and seafloor integrity. ICES Journal of Marine Science 69: 1850-1858.

Plet-Hansen, K.S., Larsen, E., Mortensen, L.O., Nielsen, J.R., Ulrich, C. 2018. Unravelling the scientific potential of high resolution fishery data. Aquatic Living Resources 31:24.

Punt, A.E., Hilborn, R. 1997. Fisheries stock assessment and decision analysis: the Bayesian approach. Reviews in Fish Biology and Fisheries 7:35-63.

Ramos, J.E., Winter, A. 2021. February bottom trawl survey biomasses of fishery species in Falkland Islands waters, 2010 – 2021. SA-2021-05. Technical Report, Falkland Islands Fisheries Department. 77 p.

Rijnsdorp, A.D., Hiddink, J.G., van Denderen, P.D., Hintzen, N.T., Eigaard, O.R., Valanko, S., Bastardie, F., Bolam, S.G., Boulcott, P., Egekvist, J., Garcia, C., van Hoey, G., Jonsson, P., Laffargue, P., Nielsen, J.R., Piet, G.J., Sköld, M., van Kooten, T. 2020. Different bottom trawl fisheries have a differential impact on the status of the North Sea seafloor habitats. ICES Journal of Marine Science 77: 1772–1786.

Roa-Ureta, R. 2012. Modelling in-season pulses of recruitment and hyperstability-hyperdepletion in the *Loligo gahi* fishery around the Falkland Islands with generalized depletion models. ICES Journal of Marine Science 69: 1403–1415.

Roa-Ureta, R., Arkhipkin, A.I. 2007. Short-term stock assessment of *Loligo gahi* at the Falkland Islands: sequential use of stochastic biomass projection and stock depletion models. ICES Journal of Marine Science 64: 3-17.

Rosenberg, A.A., Kirkwood, G.P., Crombie, J.A., Beddington, J.R. 1990. The assessment of stocks of annual squid species. Fisheries Research 8: 335-350.

Sadd, D. 2022. Observer Report 1319. Technical Document, FIG Fisheries Department. 28 p.

Shaw, P.W., Arkhipkin, A.I., Adcock, G.J., Burnett, W.J., Carvalho, G.R., Scherbich, J.N., Villegas, P.A. 2004. DNA markers indicate that distinct spawning cohorts and aggregations of Patagonian squid, *Loligo gahi*, do not represent genetically discrete subpopulations. Marine Biology, 144: 961-970.

Swartzman, G., Huang, C., Kaluzny, S. 1992. Spatial analysis of Bering Sea groundfish survey data using generalized additive models. Canadian Journal of Fisheries and Aquatic Sciences 49: 1366-1378.

Winter, A. 2014. *Loligo* stock assessment, second season 2014. Technical Document, Falkland Islands Fisheries Department. 30 p.

Winter, A. 2018. *Doryteuthis gahi* stock assessment, 1st season 2018. Technical Document, Falkland Islands Fisheries Department. 36 p.

Winter, A. 2019. Stock assessment – Falkland calamari *Doryteuthis gahi* 2nd season 2019. Technical Document, Falkland Islands Fisheries Department. 36 p.

Winter, A., Arkhipkin, A. 2015. Environmental impacts on recruitment migrations of Patagonian longfin squid (*Doryteuthis gahi*) in the Falkland Islands with reference to stock assessment. Fisheries Research 172: 85-95.

Winter, A., Juergens, L. 2014. *Loligo* stock assessment survey, 1st season 2014. Technical Document, Falkland Islands Fisheries Department. 18 p.

Winter, A., Lee, B., Shcherbich, Z., Nicholls, R. 2022. Falkland calamari (*Doryteuthis gahi*) 1st pre-season 2022 stock assessment survey. Technical Document, Falkland Islands Fisheries Department. 15 p.

Appendix
***Doryteuthis gahi* individual weights**

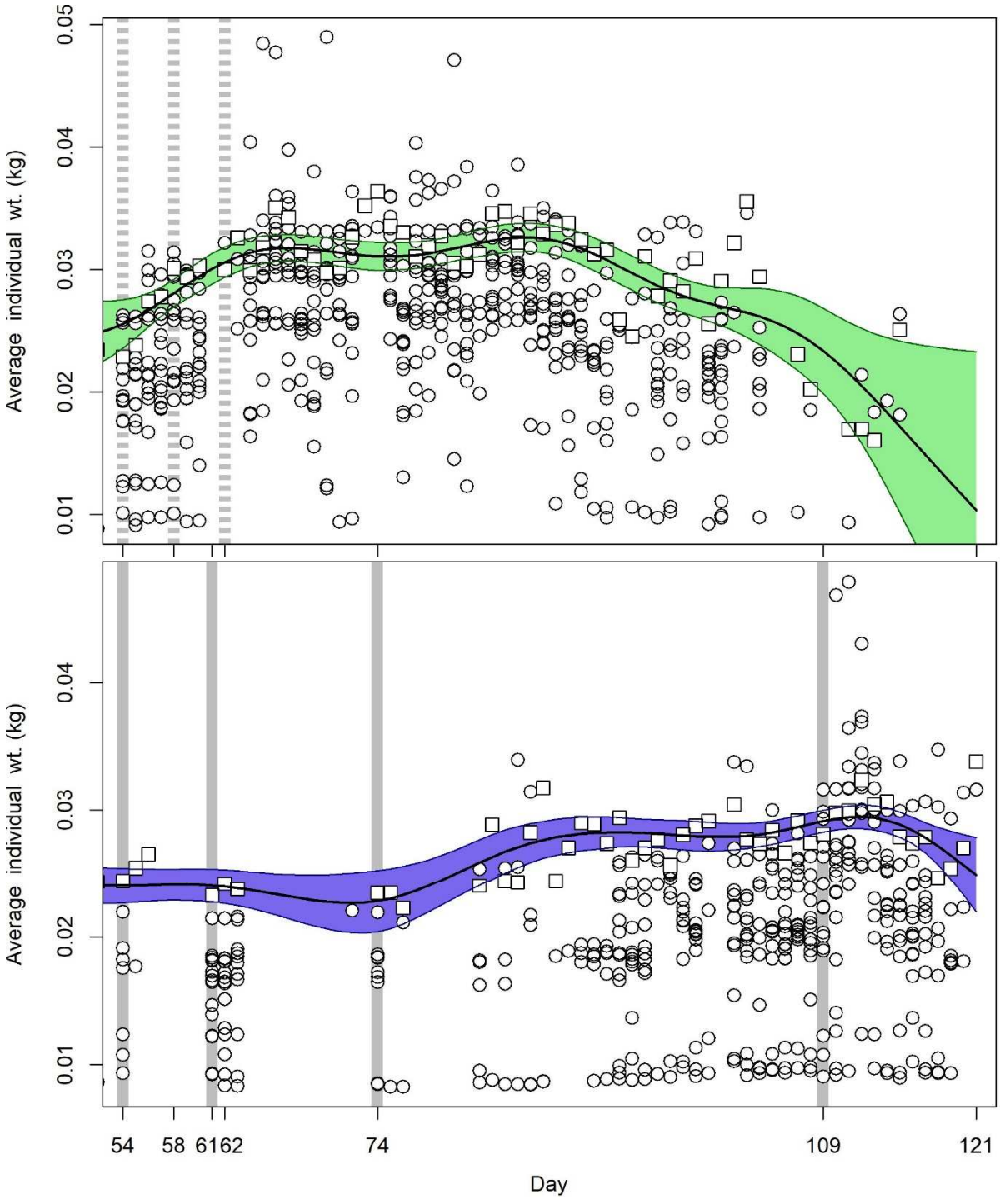

Figure A1. North (top) and south (bottom) sub-area daily average individual *D. gahi* weights from commercial size categories per vessel (circles) and observer measurements (squares). GAMs of the daily trends ± 95% confidence interval (centre lines and colour under-shading).

To smooth fluctuations, GAM trends were calculated of daily average individual weights. North and south sub-areas were calculated separately. For continuity, GAMs were calculated

using all pre-season survey and in-season data contiguously. North and south GAMs were first calculated separately on the commercial and observer data. In previous seasons, commercial data GAMs were taken as the baseline trends, and calibrated to observer data GAMs in proportion to the correlation between commercial data and observer data GAMs. However, as full observer coverage in the *D. gahi* fishery has now become standard, the algorithm was changed to make observer data the baseline, augmented by the margin by which commercial data are more frequent than observer data (if at all). For example, this season had 966 commercial fishing days (Table 1), and 925 observer days. The final GAM trend was therefore calculated as:

$$\mathrm{GAM_{Wt}} = \mathrm{Obs\ GAM_{Wt}} - \left(1 - \mathrm{pmin}\left(1, \frac{925}{966}\right)\right) \times \mathrm{mean}(\mathrm{Obs\ GAM_{Wt}} - \mathrm{Comm\ GAM_{Wt}})$$

As before, inclusion of both GAMs effected that the greater day-to-day consistency of the commercial data trends, and the greater point value accuracy of the observer data, are represented in the calculations. GAM plots of the north and south sub-areas are in Figure A1.

Prior estimates and CV

The pre-season survey had estimated *D. gahi* biomass of 47,058 tonnes (Winter et al. 2022). Hierarchical bootstrapping of the inverse distance weighting algorithm obtained a coefficient of variation (CV) equal to 10.0% of the survey biomass distribution. From modelled survey catchability, Payá (2010) had estimated average net escapement of up to 22%, which was added to the CV:

$$47{,}058 \pm (.10 + .22) = 47{,}058 \pm 32.0\% \quad = 47{,}058 \pm 15{,}059 \text{ t} \qquad \textbf{(A1)}$$

The 22% escapement was added as a linear increase in the variability, but was not used to reduce the total estimate, because squid that escape one trawl are likely to be part of the biomass concentration that is available to the next trawl.

D. gahi numbers from the survey were estimated as the survey biomasses divided by the GAM-predicted individual weight average for the survey: 0.0257 kg. The average coefficient of variation (CV) of the GAM over the duration of the pre-season survey was 3.8%, and CV of the length-weight conversion relationship (Equation **7**) was 16.1%. Joining these sources of variation with the pre-season survey biomass estimates and individual weight averages (above) gave estimated *D. gahi* numbers at survey end (day 52) of:

$$\begin{aligned} {}_{\text{prior}}\mathrm{N}_{\text{day 52}} &= \frac{47{,}058 \times 1000}{0.0257} \pm \sqrt{32.0\%^2 + 3.8\%^2 + 16.1\%^2} \\ &= 1.831 \times 10^9 \pm 36.0\% \end{aligned} \qquad \textbf{(A2)}$$

The combined catchability coefficient (q) prior was taken on day 54, the first day of the season, when 5 vessels fished in the south sub-area and 11 vessels fished in the north sub-area (Figure 3)[i]. Abundance on day 54 was discounted for natural mortality over the 2 days since the end of the survey:

$${}_{\text{prior}}\mathrm{N}_{\text{day 54}} = {}_{\text{prior}}\mathrm{N}_{\text{day 52}} \times \mathrm{e}^{-\mathrm{M}\cdot(54-52)} - \mathrm{CNMD}_{\text{day 54}} = 1.784 \times 10^9 \qquad \textbf{(A3)}$$

[i] Fifteen vessels total fished on day 54, some partially in either sub-area.

where $CNMD_{day\ 54} = 0$ as no catches intervened between the end of the survey and the start of commercial season. Thus:

$$
\begin{aligned}
{}_{prior}q &= C(N)_{day\ 54} / ({}_{prior}N_{day\ 54} \times E_{day\ 54}) \\
&= (C(B)_{day\ 54} / Wt_{day\ 54}) / ({}_{prior}N_{day\ 54} \times E_{day\ 54}) \\
&= (380.3\ t / 0.0251\ kg) / (1.784 \times 10^{9} \times 15\ \text{vessel-days}) \\
&= 0.566 \times 10^{-3}\ \text{vessels}^{-1}\ [j] \qquad \textbf{(A4)}
\end{aligned}
$$

$SD_{prior\ q}$ (Equation **4**) was calculated as ${}_{prior}q$ multiplied by its CV. $CV_{prior\ q}$ was calculated as the sum of variability in ${}_{prior}N_{day\ 54}$ (Equation **A2**) plus variability in the catches of vessels on start day 54, plus variability of the natural mortality (see Appendix section Natural mortality).

$$
\begin{aligned}
CV_{prior\ q} &= \sqrt{36.0\%^2 + \left(\frac{SD\ (C(B)_{vessels\ day\ 54})}{\text{mean}\ (C(B)_{vessels\ day\ 54})}\right)^2 + (1 - (1 - CV_M)^{(54\ -\ mid\_survey)})^2} \\
&= \sqrt{36.0\%^2 + 22.1\%^2 + 77.9\%^2} = 88.7\% \\
SD_{prior\ q} &= {}_{prior}q \times CV_{prior\ q} = 0.502 \times 10^{-3}\ \text{vessels}^{-1} \qquad \textbf{(A5)}
\end{aligned}
$$

Depletion model estimates and CV

For the south sub-area, the equivalent of Equation **2** with four N_{day} was optimized on the difference between predicted and actual catches (Equation **3**), resulting in parameters values:

$$
\begin{aligned}
{}_{depletion}N1_{S\ day\ 54} &= 0.505 \times 10^{9}; & {}_{depletion}N2_{S\ day\ 61} &= 1.247 \times 10^{9} \\
{}_{depletion}N3_{S\ day\ 74} &= 0.311 \times 10^{9}; & {}_{depletion}N4_{S\ day\ 109} &= 1.009 \times 10^{9} \\
{}_{depletion}q_{S} &= 1.736 \times 10^{-3}\ [k] & & \qquad \textbf{(A6-S)}
\end{aligned}
$$

The normalized root-mean-square deviation of predicted vs. actual catches was calculated as the CV of the model:

$$
\begin{aligned}
CV_{rmsd\ S} &= \frac{\sqrt{\sum_{i=1}^{n}\left({}_{predicted}C(N)_{S\ day\ i} - {}_{actual}C(N)_{S\ day\ i}\right)^2 / n}}{\text{mean}\left({}_{actual}C(N)_{S\ day\ i}\right)} \\
&= 3.892 \times 10^{6} / 13.105 \times 10^{6} = 29.7\% \qquad \textbf{(A7-S)}
\end{aligned}
$$

$CV_{rmsd\ S}$ was added to the variability of the GAM-predicted individual weight averages for the season (Figure A1-S); equal to a CV of 2.77% south. CVs of the depletion were then calculated as the sum:

[j] On Figure 6-left and Figure 8-left.
[k] On Figure 6-left.

$$CV_{\text{depletion S}} = \sqrt{CV_{\text{rmsd S}}^{\,2} + CV_{\text{GAM Wt S}}^{\,2}} = \sqrt{29.7\%^2 + 2.77\%^2}$$
$$= 29.8\% \quad \textbf{(A8-S)}$$

For the north sub-area, the Equation **2** equivalent with three N_{day} was optimized on the difference between predicted and actual catches (Equation **3**), resulting in parameter values:

$$_{\text{depletion}}N1_{\text{N day 54}} = 0.291 \times 10^9; \quad _{\text{depletion}}N2_{\text{N day 58}} = 0.325 \times 10^9$$
$$_{\text{depletion}}N3_{\text{N day 62}} = 0.858 \times 10^9$$
$$_{\text{depletion}}q_{\text{N}} = 3.957 \times 10^{-3}\ ^{l} \quad \textbf{(A6-N)}$$

Root-mean-square deviation of predicted vs. actual catches was calculated as the CV of the model:

$$CV_{\text{rmsd N}} = \frac{\sqrt{\sum_{i=1}^{n}\left({}_{\text{predicted}}C(N)_{\text{N day i}} - {}_{\text{actual}}C(N)_{\text{N day i}}\right)^2 / n}}{\text{mean}\left({}_{\text{actual}}C(N)_{\text{N day i}}\right)}$$
$$= 10.663 \times 10^6 / 15.394 \times 10^6 = 69.3\% \quad \textbf{(A7-N)}$$

$CV_{\text{rmsd N}}$ was added to the variability of the GAM-predicted individual weight averages for the season (Figure A1-N); equal to a CV of 2.12% north. CVs of the depletion were then calculated as the sum:

$$CV_{\text{depletion N}} = \sqrt{CV_{\text{rmsd N}}^{\,2} + CV_{\text{GAM Wt N}}^{\,2}} = \sqrt{69.3\%^2 + 2.12\%^2}$$
$$= 69.3\% \quad \textbf{(A8-N)}$$

Combined Bayesian models

For the south sub-area, joint optimization of Equations **3** and **4** resulted in parameters values:

$$_{\text{Bayesian}}N1_{\text{S day 54}} = 1.400 \times 10^9; \quad _{\text{Bayesian}}N2_{\text{S day 61}} = 3.342 \times 10^9$$
$$_{\text{Bayesian}}N3_{\text{S day 74}} = 0.394 \times 10^9; \quad _{\text{Bayesian}}N4_{\text{S day 109}} = 2.022 \times 10^9$$
$$_{\text{Bayesian}}q_{\text{S}} = 6.235 \times 10^{-4}\ ^{m} \quad \textbf{(A9-S)}$$

These parameters produced the fit between predicted catches and actual catches shown in Figure A2-S.

For the north sub-area, joint optimization of Equations **3** and **4** resulted in parameters values:

$$_{\text{Bayesian}}N1_{\text{N day 54}} = 1.768 \times 10^9; \quad _{\text{Bayesian}}N2_{\text{N day 58}} = 1.600 \times 10^9$$
$$_{\text{Bayesian}}N3_{\text{N day 62}} = 0.396 \times 10^9$$
$$_{\text{Bayesian}}q_{\text{N}} = 6.263 \times 10^{-4}\ ^{n} \quad \textbf{(A9-N)}$$

[l] Off the scale on Figure 8-left.
[m] On Figure 6-left.
[n] On Figure 8-left.

These parameters produced the fit between predicted catches and actual catches shown in Figure A2-N.

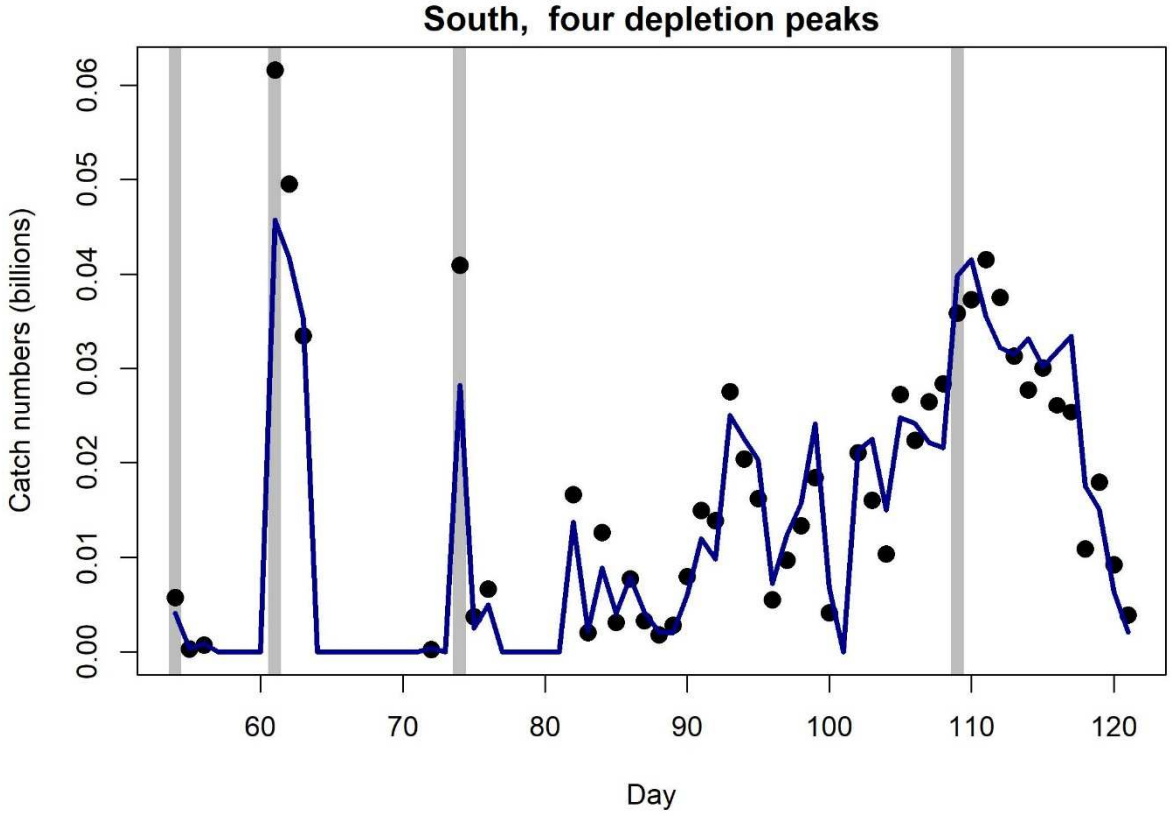

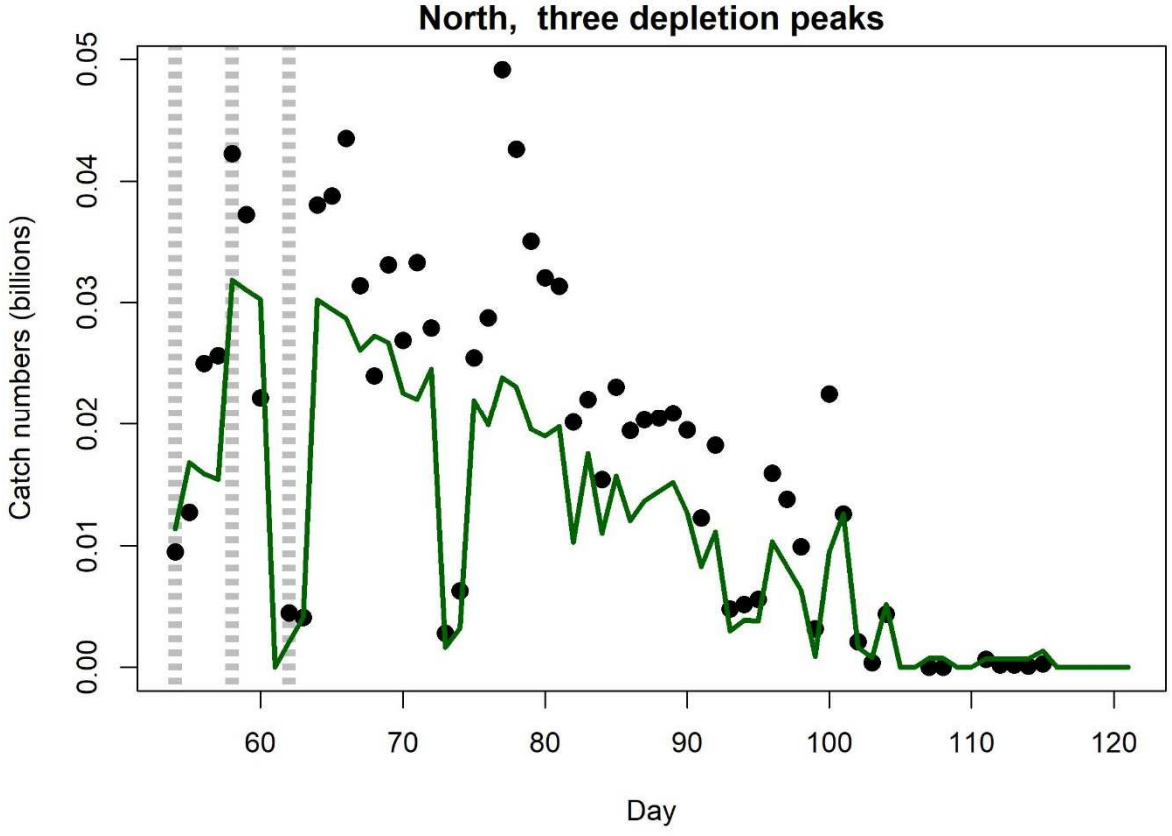

Figure A2-S [previous page – top]. Daily catch numbers estimated from actual catch (black points) and predicted from the depletion model (purple line) in the south sub-area.

Figure A2-N [previous page – bottom]. Daily catch numbers estimated from actual catch (black points) and predicted from the depletion model (green line) in the north sub-area.

Natural mortality

Natural mortality is parameterized as a constant instantaneous rate M = 0.0133 day^{-1} (Roa-Ureta and Arkhipkin 2007), based on Hoenig's (1983) log mortality vs. log maximum age regression, applied to an estimated maximum age of 352 days for *D. gahi*:

$$\log(M) = 1.44 - 0.982 \times \log(age_{max})$$

$$M = \exp(1.44 - 0.982 \times \log(352))$$

$$= 0.0133 \quad \textbf{(A10)}$$

Hoenig (1983) derived Equation **A10** from the regression of 134 stocks among 79 species of fish, molluscs, and cetaceans. Hoenig's regression obtained $R^2 = 0.82$, but a corresponding coefficient of variation (CV) was not published. An approximate CV of M was estimated by measuring the coordinates off a print of Figure 1 in Hoenig (1983) and repeating the regression. Variability of M was calculated by randomly re-sampling, with replacement, the regression coordinates 10000× and re-computing Equation **A10** for each iteration of the resample. The CV of M from the 10000 random resamples was:

$$CV_M = SD_M / Mean_M$$

$$CV_M = 0.0021 / 0.0134 = 15.46\% \quad \textbf{(A11)}$$

CV_M was aggregated over the number of days between the midpoint of the survey and the commercial season start, rather than between the end of the survey and commercial season start, as the midpoint more accurately reflects how much time has elapsed since the fishing area on average was surveyed. The midpoint of the survey was calculated as the mean day weighted by the number of survey trawls taken per day:

$$\text{mid\_survey} = \frac{\Sigma\left(\text{day} \times N_{\text{survey trawls}}|_{\text{day}}\right)}{\Sigma\left(N_{\text{survey trawls}}|_{\text{day}}\right)} = 45^{o} \quad \textbf{(A12)}$$

CV_M was thus further indexed by $1 - (1 - CV_M)$ to ensure that the value could not decrease if CV_M was hypothetically > 100%:

$$1 - (1 - CV_M)^{(\text{commercial season start} - \text{mid\_survey})} \quad \textbf{(A13)}$$

Equation **A13** is included in Equation **A5**.

[o] In common nomenclature day 45 is February 14th.

Total catch by species

Table A1: Total reported catches and discard by taxon during 1st season 2022 C-license fishing, and number of catch reports (vessel-days) in which each taxon occurred. Does not include incidental catches of pinnipeds or seabirds.

Species Code	Species / Taxon	Catch Wt. (KG)	Discard Wt. (KG)	N Reports
LOL	*Doryteuthis gahi*	56417038	57221	966
PAR	*Patagonotothen ramsayi*	555588	555538	965
HAK	*Merluccius hubbsi*	316010	17023	608
BLU	*Micromesistius australis*	149445	139840	73
ILL	*Illex argentinus*	70579	6987	387
SAR	*Sprattus fuegensis*	56855	56855	126
SCA	Scallop	40309	40309	413
CGO	*Cottoperca gobio*	32850	32850	890
KIN	*Genypterus blacodes*	31893	10161	285
BAC	*Salilota australis*	27598	4921	302
PTE	*Patagonotothen tessellata*	14900	14900	299
RAY	Rajidae	11396	9765	687
DGH	*Schroederichthys bivius*	7567	7567	467
ING	*Moroteuthis ingens*	7514	7514	435
MED	Medusae sp.	3301	3301	44
TOO	*Dissostichus eleginoides*	2824	2802	298
ALF	*Allothunnus fallai*	2253	2253	169
OCT	*Octopus* spp.	1142	1142	191
BUT	*Stromateus brasiliensis*	701	701	38
UCH	Sea urchin	445	445	56
MXX	Myctophid spp.	415	415	4
RED	*Sebastes oculatus*	400	400	29
MYX	*Myxine* spp.	307	307	31
LIM	*Lithodes murrayi*	286	286	24
SAA	*Salmo trutta*	279	279	5
GRV	*Macrourus* spp.	244	244	16
POR	*Lamna nasus*	241	241	3
SPN	Porifera	151	151	4
WHI	*Macruronus magellanicus*	113	113	33
GRF	*Coelorhynchus fasciatus*	103	103	9
MUN	*Munida* spp.	87	87	7
MUL	*Eleginops maclovinus*	49	49	19
EEL	*Iluocoetes fimbriatus*	43	43	12
LIT	*Lithodes turkayi*	31	30	7
DGS	*Squalus acanthias*	29	29	2
SEP	*Seriolella porosa*	28	28	10
COP	*Congiopodus peruvianus*	20	20	8
THA	*Thyrsites atun*	11	11	2
PAF	*Paralomis formosa*	10	10	1
CHE	*Champsocephalus esox*	10	10	5
PAT	*Merluccius australis*	8	8	2
BDU	*Brama dussumieri*	6	6	2
PRO	*Procellaria aequinoctialis*	5	3	4
THB	*Thymops birsteini*	5	5	1
NOW	*Paranotothenia magellanica*	2	2	2
Total		57753091	974975	966